ASSESSMENT OF THE IMPACTS OF LAND-USE CHANGES ON CLIMATE

Final Report

March 2025

Info crue Québec Ouranos

ASSESSMENT OF THE IMPACTS OF LAND-USE CHANGES ON CLIMATE

Final Report

March 2025

ÉQUIPE DE RÉALISATION :

Olivier Asselin, Ouranos

Martin Leduc, Ouranos

Dominique Paquin, Ouranos

Titre du projet Ouranos: Assessing the impacts of land use and land cover changes on climate using the Canadian Regional Climate Model version 5 (CRCM5)

Numéro du projet Ouranos: 706800-706802

Citation suggérée : Asselin, O., Leduc, M. et Paquin, D. (2025). *Assessment of the impacts of land-use changes on climate*. Ouranos. 69 p. + annexes.

Acknowledgments

This project was made possible thanks to the Ministère de l'Environnement, de la Lutte contre les changements climatiques, de la Faune et des Parcs (MELCCFP) as part of the government project INFO-Crue. This work was done in the scope of the Quebec-Bavaria long-term collaboration on climate change (ClimEx project). The computations of the Canadian Regional Climate Model (CRCM5) simulations were carried on the SuperMUC-NG supercomputer at the Leibniz Supercomputing Centre (LRZ) of the Bavarian Academy of Science and Humanities (project PI: Prof. Ralf Ludwig, Ludwig Maximilian University of Munich). The CRCM5 was developed by the ESCER Centre at UQAM (Université du Québec à Montréal) with the collaboration of Environment and Climate Change Canada.

This work was improved by scientific discussions with Nathalie de Noblet-Ducoudré, Diana Rechid, Édouard Davin, Alejandro Di Luca, Alexis Berg and Biljana Music, and last but not least, our stellar follow-up committee, which provided great advice and suggestions all along this project: William Gutowski, Anne-Sophie Daloz, Annie Poulin, Louis-Philippe Caron and Richard Turcotte.

The North American LUCAS ensemble came to this world thanks to the assistance of Katja Winger and Melissa Bukovsky. CRCM5 simulations and analysis would not be without the indispensable technical support of Michel Giguère, Mourad Labassi, Pascal Bourgault and Gilbert Brietzke. The North America land cover maps were the fruit of a tight collaboration with Peter Hoffmann and Vanessa Reinhart.

We are grateful for the precious work of Masters student Juliette Goulet and of summer interns Emma Peronnet and Bruno Lecavalier.

Ouranos Québec

Abstract

Context & Objectives

Human activities change climate not only by emitting greenhouse gases, but also by modifying Earth's surface. For instance, clearing a forest for crop cultivation alters the reflectivity (or albedo) and roughness of the surface as well as its ability to retain and release water through evapotranspiration. These so-called biophysical effects of land-use changes (LUC) can have a significant influence on regional climate, including temperature, precipitation, snow and wind. Paradoxically, LUC are not included in state-of-the-art operational regional climate models such as used at Ouranos.

The objectives are this project are three-fold:

1. Deepen our understanding of the biophysical effects of LUC at regional scale
2. Evaluate the performance of the fifth-generation Canadian Regional Climate Model (CRCM5) in modelling the biophysical effects of LUC
3. Lay the groundwork for the implementation of LUC in CRCM5

To achieve this, we produced an ensemble of simulations using CRCM5. The biophysical effects of LUC are assessed by running pairs of simulations with all parameters identical except for land cover. For instance, one can assess the temperature response to afforestation by comparing the average temperature from a simulation with afforested land cover versus from a simulation with the original land cover.

This project is broken down into two phases. The first phase aims to assess the sensitivity of CRCM5 to extreme LUC (i.e., the complete afforestation and deforestation of North America and Europe) and compare its response with other state-of-the-art models used in the international community. The second phase focuses on realistic scenarios consistent with the socio-economic pathways (SSPs) used by the International Panel on Climate Change (IPCC). The ensemble comprises four members (natural variability simulated in global models), two future scenarios and multiple configurations allowing to isolate the effects of greenhouse gases from those of LUC.

Results

The Land-Use and Climate Across Scales (LUCAS) initiative coordinates intercomparison projects and guides implementation of LUC in regional climate models. In the first phase of this project, we joined this European project and expanded it to North America with the support of two other regional modelling groups. We demonstrated that CRCM5 is an imperfect yet useful model to assess the biophysical effects of LUC. Indeed, CRCM5 sits well within the LUCAS ensemble, with a summertime temperature response similar to the LUCAS average and a similar albedo-driven warming pattern during the snow season. We note, however, that CRCM5 produces the most extreme winter warming amplitude of all LUCAS models. This is important to keep in mind when interpreting LUC effects in snow-covered regions and periods.

In the second phase of this project, we moved our attention to realistic LUC scenarios. Our most striking finding is the outstanding potential of forestation in mitigating summer heat waves. To illustrate this, we considered SSP1-2.6, a scenario consistent with limiting global warming to 2°C above pre-industrial levels. Thanks to large-scale forestation of Europe, heat waves are *milder* than today by 2100 for about half of the European population (Figure 1). The catch is that cooling stems from increased evaporation, which we show may cause water availability concerns in already-dry regions.

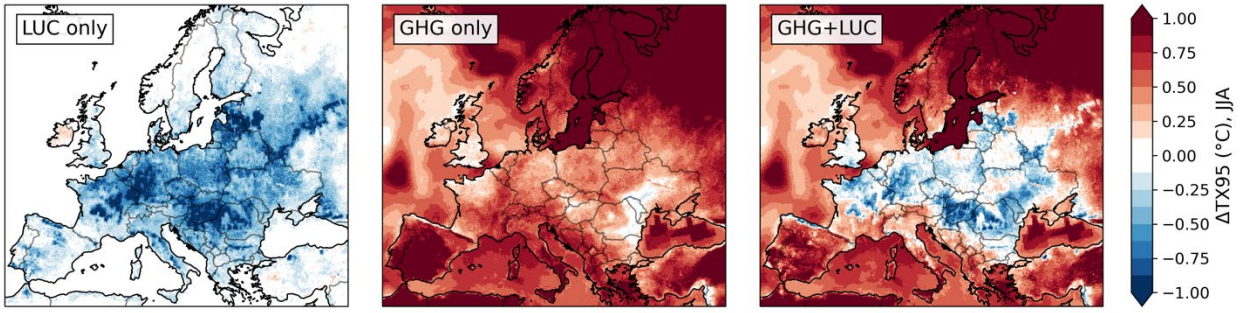

Figure 1 : LUC trump greenhouse gas emissions in mitigating summer heat extremes by the end of the century under SSP1-2.6. The three panels show the respective contributions of LUC, greenhouse gas emissions and their sum to summer heat extremes, defined by the 95th percentile of maximum daily temperature over the months of June, July and August (Asselin et al. 2024).

Another major deliverable from this project is the publication of a novel land cover dataset for North America. These freely available maps cover years 1950 to 2100 for all the main SSPs and are tailored for direct use in regional climate models. The simulation ensemble using these maps is currently under study, with a focus on the effects of LUC on the water cycle, on extreme precipitation and on the hydrology implications in northeastern watersheds.

Recommended follow-up

- Improve how surface processes are represented in the Ouranos modeling system:
    - Update land cover maps
    - Implement yearly changing land cover maps
    - Implement land surface model CLASSIC, and eventually, urban model TEB
- Pursue promising scientific avenues:
    - LUC influence on precipitation, in particular at high percentiles
    - LUC influence on renewable energy. Note, however, that we recommend waiting for the next-generation CRCM6 ensemble for studying wind energy.
    - Explore how the Ouranos modeling system can be augmented to better simulate hydrological processes
- Spread the word:
    - It is time to start a conversation with policy makers and other users about LUC
    - Begin with raising awareness about the importance of LUC for regional climate and hydrology

Contents

Acknowledgments **2**
Abstract **3**
Contents **5**
1. Introduction **7**
2. Context and objectives **8**
3. Methodology **9**
3.1. Phase I : FOREST-GRASS 10
3.2. Phase II : Realistic LUC 12
3.2.1. LUC maps 12
3.2.2. The ASIMLUC-II simulation ensemble 15
4. Results and discussion **16**
4.1. Phase I : FOREST-GRASS 16
4.1.1. Climate Response to Severe Forestation 16
4.1.1.1. Unintended benefit: soil moisture at equilibrium 18
4.1.1.2. Intended benefit: tutorial for modifying geophysical fields 18
4.1.2. Summer Internship #1: Case study on the Great Lakes Basin 19
4.1.3. Summer Internship #2: Precipitation Enhancement by Forests 19
4.1.4. Impacts of extreme LUC on hydrology 20
4.1.5. Dissemination 21
4.1.5.1. Panel on forests-climate interactions 21
4.1.5.2. Popular science article 22
4.2. Phase II : Realistic LUC 23
4.2.1. Land cover maps for realistic scenarios 23
4.2.1.1. Validation of LANDMATE and implementation in the Ouranos modeling system 24
4.2.1.2. Why not simply use the land cover maps from CCCma? 25
4.2.2. Exploratory analysis of LUC effects in Europe 26
4.2.2.1. LUC effects in ERA5-driven runs 26
4.2.2.2. Relative contributions of LUC and GHG to climatological variables of interest 29
4.2.2.3. Relative contributions of LUC and GHG to extremes 32
4.2.3. Blue in Green: Forestation in Europe under SSP1-2.6 34
4.2.3.1. Deleted section 3.3: Beyond forestation and locality 34
4.2.3.2. Diurnal cycles 35
4.2.4. LUC effects on the water cycle in North America 38
4.2.4.1. Biophysical effects of LUC under SSP1-2.6 38
4.2.4.2. Biophysical effects of LUC under SSP3-7.0 40
4.2.4.3. Beyond FOREST-GRASS 42
4.3. LUC and winds 43
4.3.1. Extreme LUC effects on wind energy in Europe 43
4.3.2. Exploratory analysis of wind in North America 44
4.3.2.1. Topography, roughness and wind 44
4.3.2.2. ASIMLUC-I: LUC effects on wind at the surface and aloft 46
4.3.2.3. ASIMLUC-II: Relative contributions of LUC and GHG on near-surface wind 48
4.3.3. Limitations 50

4.3.3.1. Effective roughness 50
4.3.3.2. Wind speed distribution and atmospheric stability 51
4.3.4. Outlook on ASIMLUC winds 52
4.3.4.1. Is it worth it pursuing the analysis of ASIMLUC wind? 52
4.3.4.2. A summary of lessons learned 53
4.4. Future Work 54
4.4.1. Opportunities for model improvement 54
4.4.1.1. Implementation of up-to-date land cover maps 54
4.4.1.2. Implementation of LUC 54
4.4.1.3. Implementation of CLASSIC 55
4.4.2. Opportunities for scientific inquiry 56
4.4.2.1. LUC and precipitation: mechanisms and extremes 56
4.4.2.2. Wind energy in Texas 56
4.4.2.3. Solar energy potential 57
4.4.2.4. Neglected LUC scenarios 57
4.4.2.5. LUC, roughness and wind in Europe 58
4.4.2.6. Internal variability 58
4.4.2.7. Hydrological studies 58
4.4.2.8. Exploring surface model parameters 59
4.4.2.9. Urban Climate 59
4.4.3. Opportunities for outreach 60
5. Conclusion 61
References 62
List of Figures 64
List of Acronyms 67

1. Introduction

According to the Intergovernmental Panel on Climate Change (IPCC) special report on Climate Change and Land (2019), humans affect nearly three quarters of the ice-free land surface. This fraction is unlikely to decrease in the future: shared socio-economic pathways (SSPs; Riahi et al. (2017)) consistent with the Paris agreement include expansions of forest and bioenergy cropland on the order of 10 million km^2, the total area of Canada. Since it is known that land-use changes (LUC) can have significant impacts on the evolution of climate, it is therefore important to include these changes in climate models for improving simulations of historical and future climate change. While state-of-the-art Global Climate Models (GCMs) use dynamic vegetation components in some experiments to account for the two-way interactions between the surface and the atmosphere, regional climate models (RCMs) generally do not include this component. This contrasts with the fact that LUC can be particularly important at the regional scale where surface heterogeneity can directly affect local climate and its projected changes in the future.

LUC impact climate by modulating greenhouse gas (GHG) emission and sequestration, surface albedo, evapotranspiration and surface roughness (Perugini et al., 2017). For instance, replacing grassland with a forest is likely to increase carbon sequestration during tree growth, lower albedo and thus increase sunlight absorption, increase evaporative cooling via enhanced transpiration, and increase surface roughness and thus possibly cloud cover and precipitation. The net climate impact of these processes is not clear as their relative influence depends on surface characteristics, geographical location and season. This project aims to investigate these questions, with a focus on the biophysical (non-GHG) effects of LUC influencing albedo, evapotranspiration and surface roughness. Although these biophysical impacts of LUC likely affect local climate in similar proportion to the global GHG forcing (de Noblet-Ducoudré et al., 2012), they are comparatively much less studied and understood.

Davin et al. (2020) presented results from the first phase of the Land-Use Across Scales (LUCAS) project, an international effort to integrate LUC in RCMs and quantify their biophysical impacts. They compared the climate response in different combinations of RCMs and land surface models (LSMs) to extreme deforestation and afforestation in Europe. In wintertime, the models tend to agree on a warming effect of afforestation due to a lowered albedo (forest tend to be darker than other land types, and more likely to hide snow). However, the inter-model spread in summertime is alarming, with some models predicting widespread warming and others widespread cooling. There is thus a pressing need to understand the source of this inter-model divergence and reduce the uncertainty in predicting the climate impacts of LUC.

2. Context and objectives

To recapitulate, land-use changes (LUC) can modify climate by emitting or absorbing greenhouse gases (biochemical effects) and by altering the exchanges of energy and water between the atmosphere and Earth's surface (biophysical effects). Biophysical effects of LUC can have both local (e.g. change of albedo due to reforestation warms the surface) and non-local (e.g. decreased evapotranspiration from deforestation reduces downwind precipitation) impacts on climate. These effects are highly complex and remain at the cutting edge of scientific inquiry. While state-of-the-art global climate models (GCMs) typically include the biophysical effects of LUC, to this day no operational regional climate model (RCM) takes these effects into account. This is paradoxical, because biophysical effects of LUC can exert a dominant influence at the regional scale.

This Assessment of the Impacts of Land-Use Changes on Climate (ASIMLUC) aims to tackle three broad, tightly-coupled objectives:

1. Deepen our understanding of the biophysical effects of LUC at regional scale
2. Evaluate the performance of the Canadian Regional Climate Model (CRCM5) coupled to the Canadian Land Surface Scheme (CLASS) in modelling the biophysical effects of LUC
3. Lay the groundwork for the implementation of LUC in operational RCMs

ASIMLUC is broken down into two phases. Its first phase, also called FOREST-GRASS, aims to assess the sensitivity of CRCM5-CLASS to extreme LUC, i.e., complete afforestation and deforestation, and compare its response with other combinations of RCMs and land surface models (LSMs). Its second phase focuses on realistic LUC scenarios consistent with SSP1-2.6 and SSP3-7.0, and compares the biophysical effects of LUC to the better-studied effects of greenhouse gases (GHGs).

3. Methodology

Both phases of ASIMLUC are exclusively based on simulated climate data. The basic principle of the methodology is illustrated in Figure 2: run a pair of RCM simulations which are identical except for a parameter interest (say, land cover), and compute the difference in the variable of interest between the pair of simulations. For instance, in FOREST-GRASS (Phase I), we ran two CRCM5 simulations forced by identical sea and atmospheric conditions from the ERA interim reanalysis: one fully covered with trees (FOREST), and another fully covered in grasses (GRASS). The effect of forests on, say, temperature can thus be approximated as the climatological temperature in the FOREST simulation that in the GRASS simulation.

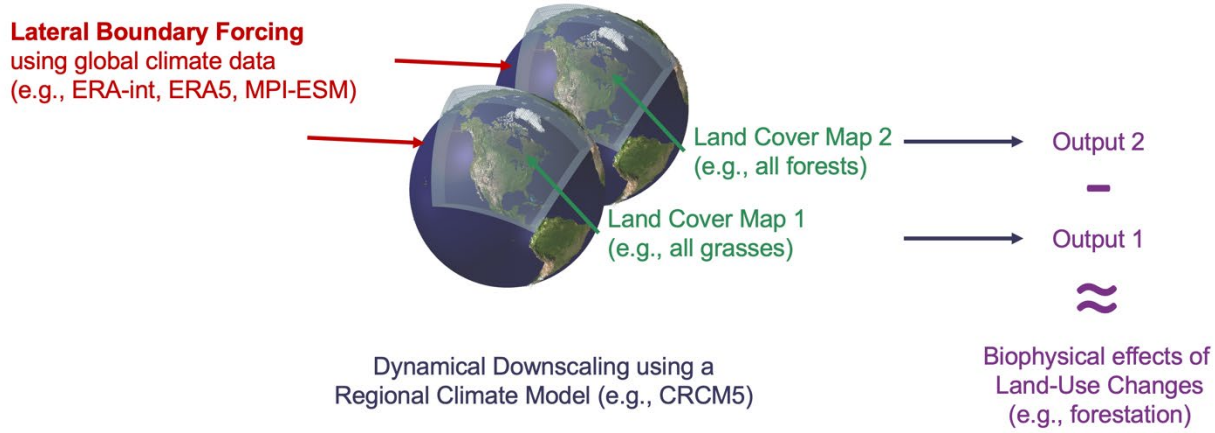

Figure 2 : Illustration of the methodology used in this project. Global climate data, which may come from reanalyses or global climate models, is downscaled dynamically over a given continent and period. Regional climate simulations with different configurations (e.g., land cover maps) are compared to assess the effect of this change on a variable of interest (e.g., temperature).

Similarly, one can assess the impacts of GHG by comparing pairs of simulations with identical land cover but different GHG concentrations, as we do in ASIMLUC-II. Note that internal variability, the inherent chaotic noise in the climate system, may also masquerade as LUC or GHG effects. To keep this noise in check, we repeat simulations with the same RCM configuration but with different members of the GCM ensemble used in ASIMLUC-II. In other words, our method is to generate an ensemble of RCM simulations in order to cleanly isolate the climate effects of LUC, GHG and internal variability.

Both phases of ASIMLUC use the same configuration of CRCM5 (Šeparović et al. (2013), Martynov et al. (2013)) and CLASS v3.5 (Verseghy (1991), Verseghy et al. (1993)). The only difference between simulations are the forcing data (ERA-int in phase I vs ERA5 and MPI-ESM in phase II), land cover maps, and spatial resolution (0.44 degree in phase I vs 0.11 degree in phase II). Table 1 in Asselin et al. (2022) provides a more complete description of the aspects of the model relevant to the experiments. The complete technical documentation of the ASIMLUC dataset is available in the annex (/Dataset Documentation/).

Let’s now look at the particularities in the methodology for each phase.

3.1. PHASE I : FOREST-GRASS

In the first phase of ASIMLUC, called FOREST-GRASS, we joined the leading international effort to improve understanding of the biophysical effects of LUC and include these effects in operational RCMs: the LUCAS Flagship Pilot Study (FPS) of the Coordinated Regional Downscaling Experiment (CORDEX). The LUCAS team designed the FOREST-GRASS protocol, whereby participating modeling centers would test the sensitivity of their RCM/LSM to extreme afforestation and deforestation. Global maps were created with all vegetation replaced by trees (FOREST map) or grasses (GRASS map), keeping glaciers and desert unchanged (Figure 3). These maps thus represent a theoretical maximum for afforestation and deforestation.

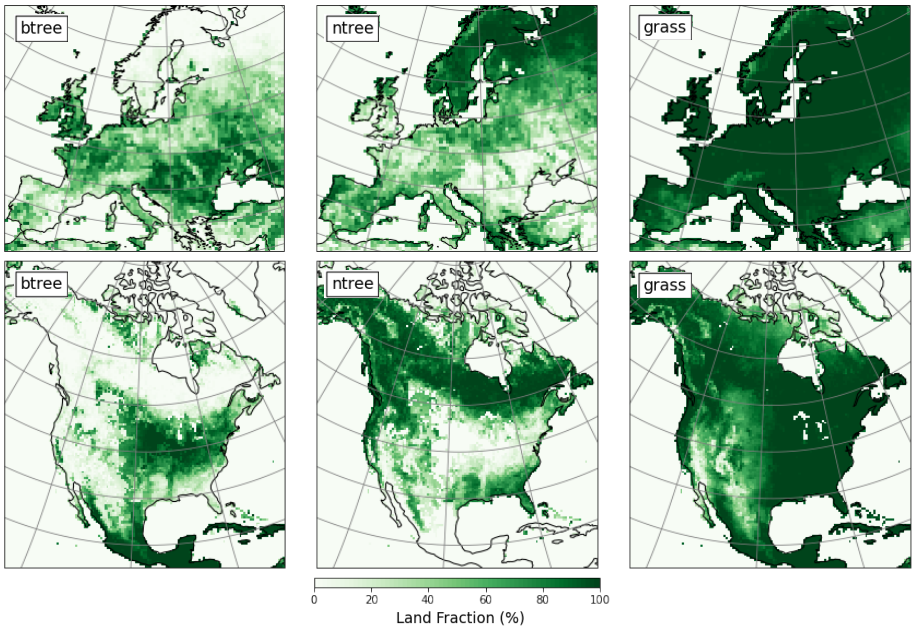

Figure 3: Land cover maps for ASIMLUC-I: FOREST and GRASS.

Each modeling center ran a pair of reanalysis-forced regional climate simulations using the FOREST and GRASS maps, such that the difference between simulated climates corresponds to the biophysical effects of extreme LUC (see Figure 2). A third optional control simulation, sometimes referred to as EVAL, was produced using the unaltered vegetation map.

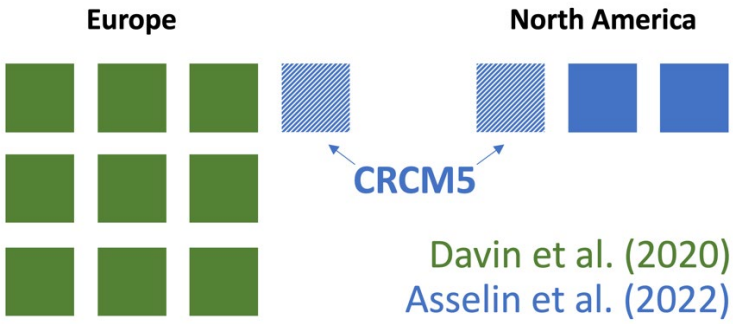

Figure 4: The expanded LUCAS simulation ensemble. Each square corresponds to a trio of simulations (FOREST, GRASS and control) for a unique RCM/LSM combination. Green squares depict the original LUCAS ensemble described in Davin et al. (2020). Blue squares depict the ensemble produced in the first phase of ASIMLUC.

In addition to participating in the original LUCAS experiment, which focused on Europe, we initiated a North American version of LUCAS to assess the transferability of the RCM climate responses on a different continent (see Figure 4). Two other modeling groups, UQAM and NCAR, joined this effort and tested the sensitivity of their model to extreme LUC in North America. In the light of Davin et al. (2020), such model intercomparison is essential to learn about the CRCM5-CLASS performance in its simulated response to idealized LUC before simulating climate projections with finer-grain, more realistic LUC forcing of the second phase.

3.2. PHASE II : REALISTIC LUC

In the second phase of ASIMLUC, we assess the relative contributions of the biophysical effects of LUC and GHG concentrations on regional climate in more plausible scenarios. We consider two shared socio-economic pathways, SSP1-2.6 and SSP3-7.0, respectively known as the 'sustainability' and 'regional rivalry' scenarios. These two scenarios, in addition to being recommended by the CORDEX community and LUCAS in particular, exhibit among the most important LUC signals and span a wide GHG forcing range. For the comprehensive reasoning underlying the choice of scenario, the reader is referred to the annex (/Extras/Choice of SSP/).

To simulate the effects of realistic LUC, the first step is to generate land cover maps that can be digested by CRCM5-CLASS and which represent land conditions in the past, present and future. This was a major undertaking and constitutes the first deliverable of ASIMLUC-II. Section 4.2.1 is dedicated to describing the process in more detail. For now, we discuss the resulting land cover maps to be used in the ASIMLUC-II ensemble (Figure 5 and Figure 6).

3.2.1. LUC maps

The two chosen scenarios differ significantly both in terms of their GHG and LUC forcings. Under SSP1-2.6, ambitious climate mitigation efforts imply rapid cuts in GHG emissions and large-scale reforestation and afforestation (herein combined as forestation). For both continents, the spatially-averaged signal (see Figure 7) is relatively similar: more broadleaf and needleleaf trees at the expense of grasses and shrubs. SSP3-7.0, on the other hand, is a high-emission scenario, and its LUC signal is more complex. In North America, there are large-scale forest clearings to make room for cropland. In Europe, the signal is one of 'shrubification' of cropland with change in tree area.

One might be tempted to think of LUC in SSP1-2.6 and SSP3-7.0 as realistic, or at least technically-feasible versions of FOREST and GRASS, respectively. While this is a decent first-order mental model, there are important distinctions to bear in mind:

- As the name suggests, FOREST and GRASS only differ by their fractional coverage of trees and grassland. Neither simulation contains cropland, shrubland or urban area. It turns out that changes in these land cover categories, notably cropland and shrubland, matter a lot in some scenarios and regions (more on this in sections 4.2.3 and 4.2.4)
- SSP1-2.6 in both North America and Europe does indeed look like a more plausible version of the FOREST scenario (see Figure 7). Note, however, that there are large regional variations in cropland area, despite weak spatially-averaged changes. There are also significant drops in shrubland areas, which turn out to also be important (more on this in sections 4.2.3).
- While SSP3-7.0 in North America superficially looks like a technically-feasible version of GRASS, we note that large-scale clearing of forests happens mostly make room for cropland, not grassland. This apparently benign distinction is crucial (see discussion in section 4.2.4).
- SSP3-7.0 in Europe is complex and shares little with either FOREST or GRASS ideal cases.

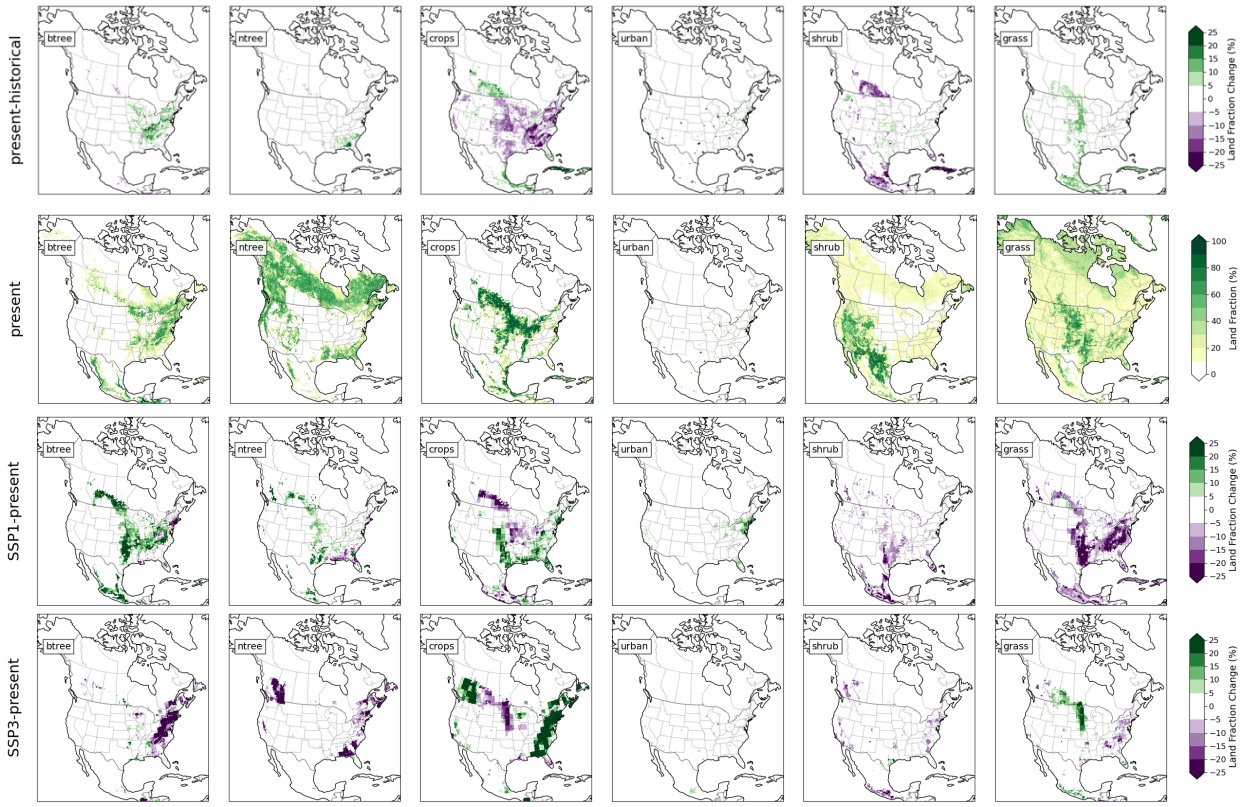

Figure 5: LANDMATE land cover maps in the present (2015), and LUC between 2015 and 2100 for SSP1-2.6 and SSP3-7.0.

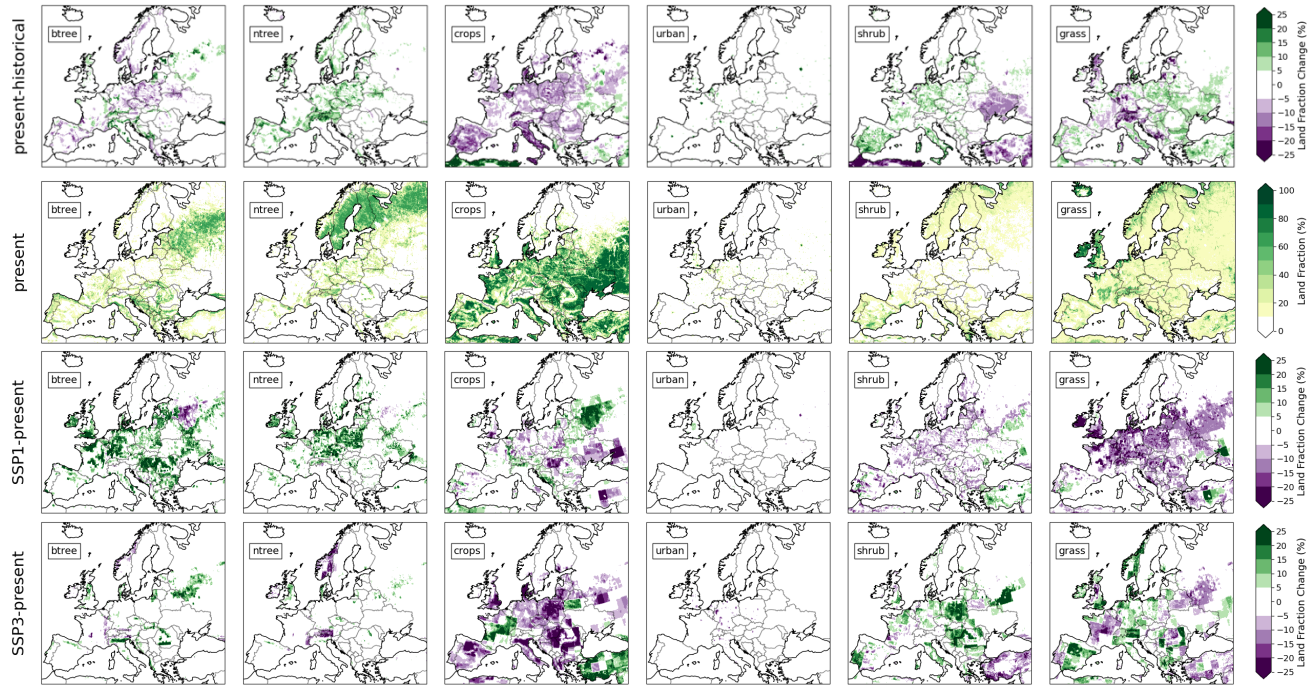

Figure 6 : LANDMATE land cover maps in the present (2015), and LUC between 2015 and 2100 for SSP1-2.6 and SSP3-7.0.

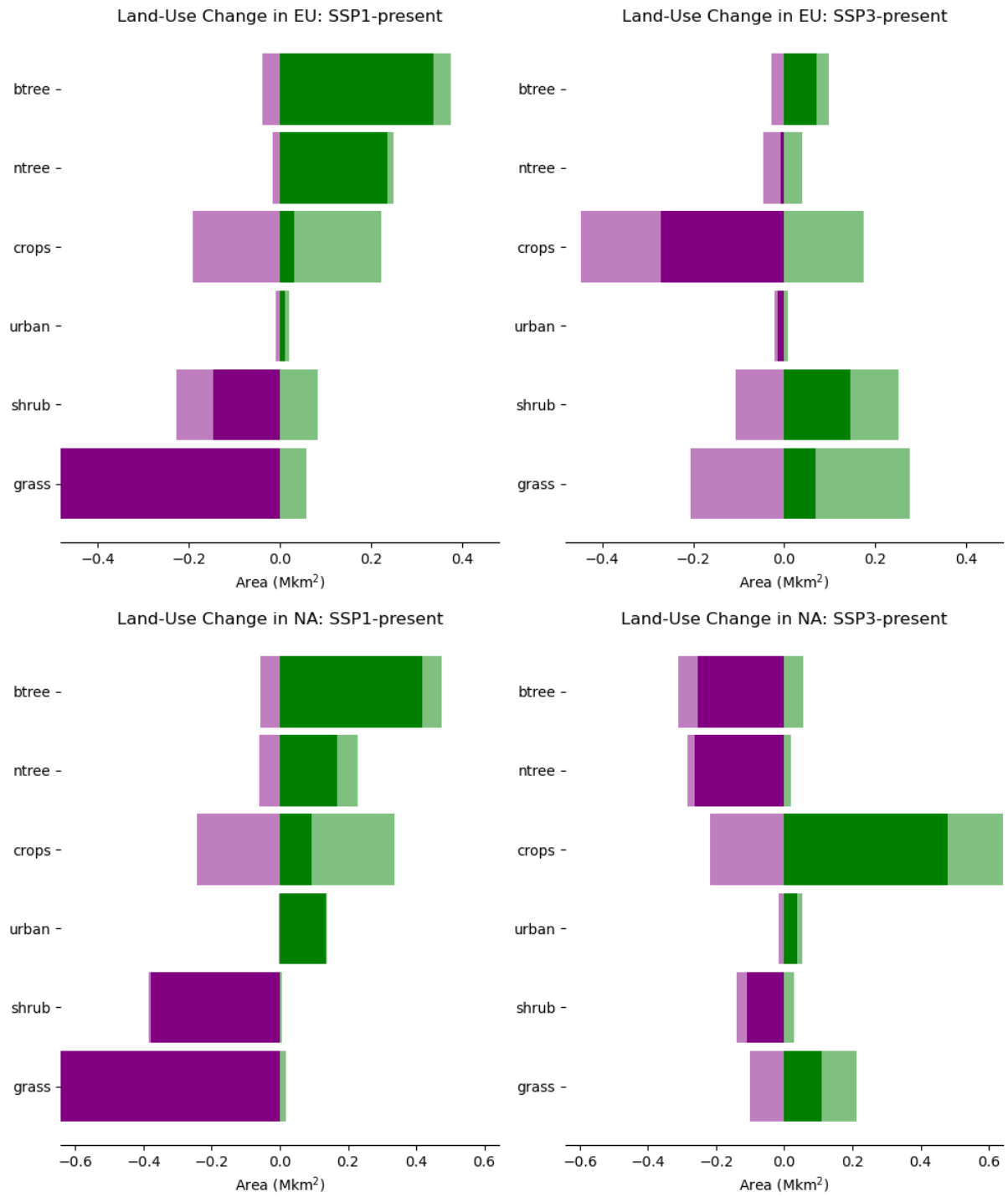

Figure 7 : Spatially-integrated land-use changes between 2015 and 2100 for both continents and both scenarios. The bar graphs show the sums of all positive (pale green) and all negative (pale purple) changes as well as the net change (dark green or purple).

3.2.2. The ASIMLUC-II simulation ensemble

The ASIMLUC-II ensemble consists of 48 regional climate simulations across two continents, of which 40 are driven by the Max Planck Institute Earth System Model (MPI-ESM) and 8 are driven by the ERA5 reanalysis (see Figure 8, which summarizes simulations for one continent). The ERA5 ensemble allows us to assess the effects of LUC under current climate conditions, whereas the MPI-ESM ensemble allows us to assess the effects of LUC under future climate conditions, as well as the effects of GHG and internal variability.

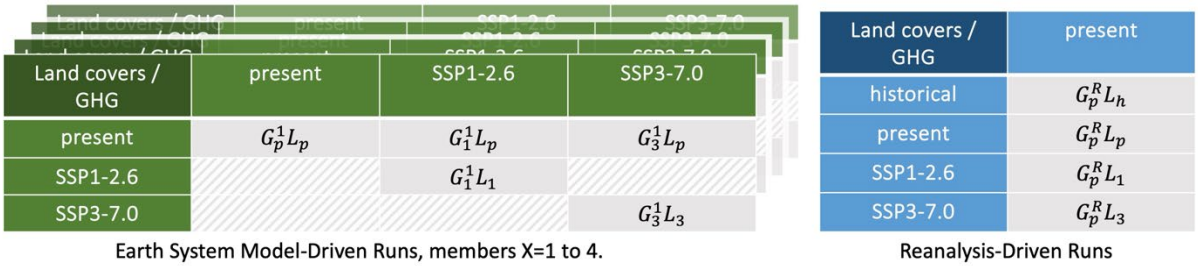

Figure 8: Simulation ensemble for ASIMLUC-II (for both North America and Europe). The four green tables represent the ensemble forced by the four MPI-ESM members. There are five model configurations with different combinations of GHG and land covers, times 4 members. The blue table represents the ERA5-driven ensemble.

Simulations in present climate span years 1979 to 2020, but the climatological period analyzed is 1986-2015. Future simulations span years 2064 to 2100. Due to technical difficulties with the host supercomputer at the Leibniz-Rechenzentrum (LRZ), a few simulations in the North America ensemble were not fully completed (see details in the annex: /Dataset Documentation/). For this reason, the future climatology must be averaged over 2070-2099 for the North America ensemble. All analysis of Europe simulations so far focuses on the year range 2071-2100.

With CRCM5, GHG concentrations are specified yearly for each scenario. Land cover, on the other hand, is static for each simulation. Historical, present and future land covers are respectively taken at years 1950, 2015 and 2100.

4. Results and discussion

Half a petabyte of climate simulation data was generated over the two phases of ASIMLUC, and several distinct subprojects involved mining this dataset for various aims. This section is an attempt to summarize the most salient features uncovered so far. To maximize scientific impact, the bulk of major results were packaged in scientific papers. At the time of writing two main peer-reviewed papers were published in scientific journals, one for each phase, and we briefly summarize them below. There were also two summer internships and one Masters project directly working with the dataset, which have yielded interesting results but have not (yet) led to publications. In addition, exploratory work connecting ASIMLUC with a new Ouranos project on wind was deemed relevant for this report and will be discussed briefly.

4.1. PHASE I : FOREST-GRASS

4.1.1. Climate Response to Severe Forestation

The bulk of the analysis for ASIMLUC-I simulations is summarized in the scientific paper "*On the Intercontinental Transferability of Regional Climate Model Response to Severe Forestation"*, by O. Asselin et al., published in 2022 in the journal *Climate* (see Annex/Publications/Scientific Papers/).

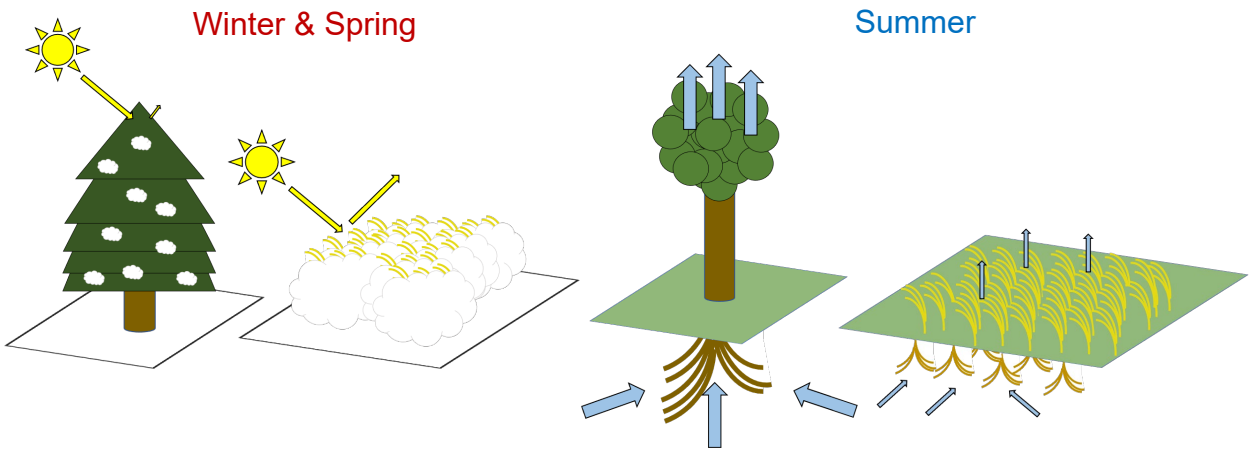

Figure 9: Illustration of main mechanisms driving the temperature response to extreme LUC. Left: albedo-driven warming in winter and spring. Right: evapotranspiration-driven cooling in the summer.

In essence, Asselin et al. (2022) present the main results of the North American extension of the FOREST-GRASS experiment (Figure 4). We start by showing how extreme forestation alters the surface energy budget and temperature in CRCM5-CLASS over both Europe and North America. In wintertime, snow masking by evergreen needleleaf trees causes a large drop in albedo, which translates into a significant increase in net shortwave radiation and hence warming (Figure 9). The effect is even stronger during spring, where forestation can increase 2-meter temperature by more than 10 degrees. Interestingly, we find that this warming effect is more pronounced in North America than in Europe, because evergreen needleleaf forests populate lower, sunnier latitudes in North America.

Variable of interest	CRCM5 response over NA/EU	CRCM5 vs LUCAS ensemble
Winter/spring temperature	Widespread **winter and spring warming** due to snow masking at high-latitudes. Needleleaf afforestation would cause stronger biophysical warming in NA than EU, because needleleaf trees populate lower hence sunnier latitudes in NA	CRCM5 has a **consistent but more pronounced** response than other models
Summer temperature	**Dipolar summertime response:** albedo-driven warming over northern needleleaf forests, evapotranspiration-driven cooling over southern broadleaf forests	CRCM5 has a response **resembling the ensemble mean**, but there is **wide inter-member divergence**
Summer Precipitation	**Forestation enhances precipitation** (mechanisms remain to be clarified)	**No clear consensus** regarding the precipitation response in the ensemble

Figure 10 : Summary of the CRCM5-CLASS response to extreme afforestation/deforestation and comparison with LUCAS ensemble, based on Asselin et al. (2022).

When comparing the albedo-driven wintertime warming to other RCM/LSM in Europe, we find that CRCM5-CLASS is among the most sensitive models to forestation (Figure 10). In the North American ensemble, CRCM6-GEM5 produces a very similar response to forestation, while WRF-NOAH simulates no difference in net shortwave radiation in snow-covered region (which is highly questionable after realizing that snow completely covers a tree if snow depth is more than 8 cm).

In the summertime, the CRCM5-CLASS response is a more complicated mix of albedo-driven warming over northern needleleaf forests and evapotranspiration-driven cooling over southern deciduous forests (Figure 9). A similar response is seen in CRCM6-GEM5-CLASS, while WRF-NOAH produces a completely different signal. The original LUCAS ensemble also exhibits strong inter-model divergence in the summertime temperature response (Figure 10). A relatively reliable pattern nevertheless emerges whereby the evaporative fraction (the ratio of turbulent fluxes due to latent heat fluxes) is strongly anticorrelated with the temperature. In other words, even if the summertime temperature response to forestation of RCMs/LSMs differs widely, models that simulate more evapotranspiration tend to simulate decreased summertime temperature. Curiously, the CRCM5-CLASS summertime dipole-shaped temperature response in Europe resembles the average of all LUCAS model responses. Of course, such an average is not so meaningful given the strong inter-model divergence, but it does indicate that CRCM5-CLASS sits well within the LUCAS ensemble in terms of its summertime response. This gives us confidence that CRCM5-CLASS is an imperfect but trustworthy tool to examine the biophysical effects of LUC.

4.1.1.1. Unintended benefit: soil moisture at equilibrium

The first (unintended) benefit of ASIMLUC-I is the improvement of soil moisture modeling used in the Ouranos operational simulations. In short, analysis of the water budget in the FOREST-GRASS simulations revealed that the initial condition of soil moisture, which is the same used for operational simulations at Ouranos, lacks moisture in the deepest soil layers. While the first few meters of soil are relatively well coupled to the atmosphere and quickly adjust to different climatic conditions, soil moisture in the deeper (>2 meters) layers evolves much more slowly. As a result, vertically-integrated soil moisture increases for the whole duration of century-long operational simulations, as moisture slowly percolates down to the deepest model layers. While this may not significantly influence atmospheric processes, which primarily depend on the top soil, it is a serious concern for any application of the Ouranos operational simulations in which deep soil moisture is relevant.

An internal report (see annex: /Extras/Water at Equilibrium) was written on the problem and how to fix it, namely by using the soil moisture profile obtained after running the control version of the FOREST-GRASS experiment for over 40 years. This allowed an important correction of future operational simulations at Ouranos, with significant benefits for applications in hydrology, agriculture, water management, ecological impacts, etc.

4.1.1.2. Intended benefit: tutorial for modifying geophysical fields

Another benefit of ASIMLUC is to minimize the multiple rounds of trial-and-error required when using the “legacy” programs to manipulate the CRCM5 binary format. Time spent working with the r.diag library led to the creation of internal documentation on how to modify the geophysical fields (such as land cover maps) for preparing CRCM5 (and CRCM6-GEM5) simulations (see annex: Extras/Geophysical Fields Tutorial/).

4.1.2. Summer Internship #1: Case study on the Great Lakes Basin

A first summer internship was proposed to study the impacts of extreme forestation in the Great Lakes region. The analysis, summarized in an internal report available in the annex (/Publications/Summer Internship Reports/), was carried out by Emma Peronnet under the supervision of O. Asselin and B. Music during the summer of 2022.

In summary, analysis suggests that forestation of North America increases the temperature, evapotranspiration, and precipitation over the Great Lakes Basin. The presence of forests reduces peak lake ice fraction by about half and expedites ice melting by about one month (see figure 14 of the report). The lake albedo is therefore lower and extra shortwave radiation warms the lakes. Evaporation from the lakes is also found to be higher during summer and fall (figure 19), although the precise mechanism could not be identified with certainty.

The FOREST world has less snow accumulation, and snowmelt occurs about a month earlier than in the GRASS world. Related to this, the spring surface run-off peak is greatly diminished due to forests (figure 40). Interestingly, FOREST receives more precipitation on average, and therefore the deep run-off is increased on average. It is hypothesized that forests may be beneficial to flood management by smoothing the monthly run-off signal, at least in the Great Lakes Basin.

4.1.3. Summer Internship #2: Precipitation Enhancement by Forests

A second summer internship was proposed to study the mechanisms by which forestation influences precipitation, in particular summer precipitation in North America. The analysis, summarized in an internal report available in the annex (/Publications/Summer Internship Reports/), was carried out by Bruno Lecavalier under the supervision of O. Asselin and B. Music during the summer of 2023.

On average, forests enhance both climatological and extreme precipitations in the FOREST-GRASS experiment, although there is considerable regional and temporal variability in the sign and amplitude of the signal. The roles of several interlinked mechanisms were examined. It was found that forests drive increases in the convective available potential energy (CAPE), which is directly associated with enhanced convective precipitation. Forests also tend to favor evapotranspiration, which contributes to humidifying the atmosphere. However, regions where strong evapotranspiration occurs (such as the eastern U.S. broadleaf forests) tend to be associated with greater atmospheric stability and decreased moisture convergence, such that precipitation is not enhanced directly over the source of additional moisture. In sum, while trees enhance precipitation on average in time and over the continent, the effects are non-local and more work is needed to pinpoint the exact mechanisms underlying precipitation enhancement.

4.1.4. Impacts of extreme LUC on hydrology

Ongoing work at the École de technologie supérieure (ETS) uses ASIMLUC-I data in conjunction with hydrological models to assess the effects of extreme LUC on hydrology. The main results of this exercise are outlined in a paper to be submitted to the Journal of Hydrology: "*Impacts of severe land use changes on the hydrology of Eastern North American watersheds*" by Siavash Pouryousefi Markhali, Mariana Castañeda Gonzalez, Annie Poulin, Jean-Luc Martel, Richard Arsenault, François Brissette, Olivier Asselin and Richard Turcotte (see in annex: /Publications/Scientific Papers/).

In this paper, the authors use ERA5 along with the FOREST, GRASS and EVAL simulations to drive hydrological simulations with the distributed physically-based hydrological model HYDROTEL over 89 watersheds of Eastern North America. In general, afforestation tends to advance and diminish spring peak flows, while conversion to grasslands delays and magnifies them.

Most interestingly, it is found that extreme LUC affect spring peak flows principally via changes to temperature and precipitation. In other words, extreme LUC effects on evapotranspiration and snow dynamics, which are dealt with internally in HYDROTEL, have less impact on hydrology than the LUC-induced changes to temperature and precipitation data fed by CRCM5. This is made clear by so-called "wrong" simulations, where FOREST and GRASS climate data is fed to hydrological models which retain GRASS and FOREST land cover, respectively. Swapping climate and land cover data shows that the later exerts the strongest influence. Additional simulations with hydrological model WaSiM show even less "direct" response to land cover: the difference in the hydrological response stems entirely from feeding "climate" data.

An interesting future avenue of inquiry would be to compare the output of these HYDROTEL and WaSiM simulations to the hydrology produced by CLASS. It is expected that evapotranspiration and snow dynamics are better simulated in CLASS than these hydrological models. We discuss this possibility in section 4.4.2.7.

4.1.5. Dissemination

The role of forests in mitigating climate change is a frequently discussed subject in the public sphere. In an effort to reach out and share the results of ASIMLUC-I with the wider public, two disseminations activities were implemented: a panel at the 2022 Ouranos Symposium, and the publication of a popular science article.

4.1.5.1. Panel on forests-climate interactions

The 2022 Ouranos Symposium featured a panel titled "Interaction Forêts-Climat: Séquestration Carbone et Autres Effets", which was moderated by O. Asselin. Below we list some of the highlights from this discussion.

- Dominic Cyr, expert on the carbon budget of forests at Environment and Climate Change Canada, shared how LUC and forestry practices on managed lands are actually *not* included in Canada's carbon accounting, which reports net emissions of roughly 700 Mt CO2 annually. In addition, when accounting for natural disturbances like wildfires and pest infestations, managed forests become a net source of carbon emissions, contributing between 100-200 Mt CO2 to the atmosphere.

- Claude Villeneuve, biologist and founder of Carbone Boréal, expanded on the role of the organization, emphasizing that it goes beyond mere tree planting. They focus on reforestation in areas that would not naturally regenerate, thus contributing to both carbon sequestration and advancing scientific research in forestry. He also touched on the strategic planting of larches at various latitudes, aimed at optimizing albedo effects, which can influence local climate conditions more significantly than CO_2 impacts.

- Nathalie de Noblet-Ducoudré, scientist and expert in modelling of land-use changes and their effects on climate, reiterated the importance of considering biophysical effects, which can sometimes overshadow the carbon-related impacts of forests at a local scale. This perspective underscores the complexity of forest-related climate strategies, where biophysical interactions must be carefully balanced with carbon management goals.

- Évelyne Thiffault, director of the Montmorency Forest, an experimental laboratory for forestry, discussed opportunities within the forestry sector, suggesting that partial cutting could benefit both industry and natural ecosystems by promoting healthier forest regeneration. She also advocated for the valorization of wood products and the use of wood residues for bioenergy, pointing towards a sustainable cycle that enhances the value of forest resources while contributing to energy generation.

4.1.5.2. Popular science article

A popular science article discussing the multifaceted role of trees in combating climate was published in *Climatoscope*, a yearly journal discussing climate-related topics in an accessible prose. The article is freely accessible online (French only; see annex: /Publications/Dissemination/).

The article begins by referencing political endorsements for large-scale tree planting campaigns, like Justin Trudeau's 2019 pledge to plant two billion trees in Canada by 2030 and similar international efforts supported widely across political lines due to their public appeal. It emphasizes that while trees are universally beloved and politically favorable, their actual utility in mitigating climate warming needs careful consideration.

Trees absorb CO_2 through photosynthesis, a process that makes them valuable as carbon sinks; however, the storage is only temporary, lasting until the tree dies and potentially returns much of the stored carbon to the atmosphere. Moreover, the article discusses how forests influence the climate beyond simple carbon sequestration. Through changes in albedo, evapotranspiration, and surface roughness, forests can alter local climates significantly. These biophysical properties, however, can lead to warming under certain conditions, particularly at higher latitudes where dark forests can reduce the Earth's albedo by covering snow.

The overarching message of the article is a call for a nuanced appreciation of forestation in climate strategies. While planting trees can indeed sequester carbon, the biophysical effects they induce—such as changes in albedo, evapotranspiration, and roughness—can sometimes negate these benefits, especially in colder regions. The article concludes by stressing that while forestation is a valuable tool in achieving carbon neutrality, it cannot replace the necessity of reducing greenhouse gas emissions and should be integrated thoughtfully with broader climate change mitigation strategies.

4.2. PHASE II : REALISTIC LUC

Phase II involved the production of a 48-simulation ensemble at 0.11° resolution, totalizing nearly half a petabyte of data. The land cover maps to be used for North America were non-existent when phase II began. Hence, the first step was to generate them (section 4.2.1). This process took way longer than expected, and the Europe simulation ensemble was completed before the North America ensemble was even started. As such, simulations over Europe benefited from the first in-depth analysis. We were initially on our way to publishing a more lengthy, descriptive paper based on this analysis (section 4.2.2). However, following discussions with our collaborators, it was deemed more pertinent to frame the paper around the most important aspects of LUC effects in Europe: attenuation of heat waves and the consequences for water availability. The resulting paper, published in *Environmental Research Letters*, is summarized and expanded in section 4.2.3. An ongoing Masters project, expected to be concluded by early 2025, focuses on the effects of realistic LUC on the water cycle in North America (section 4.2.4).

4.2.1. Land cover maps for realistic scenarios

Land cover maps for the recent past, present and various future scenarios are needed to assess the effects of realistic LUC. For the second phase of the LUCAS project (not to be confused with ASIMLUC-II), Reinhart et al. (2022) and Hoffmann et al. (2023) generated yearly plant functional type (PFT) maps from 1950 to 2100 for several SSPs over a 0.1-degree grid covering Europe. The primary source of data for the present land cover map, the so-called LANDMATE[2] map, comes from the recent European Space Agency Climate Change Initiative (ESA-CCI) satellite product, but several other secondary sources are used to maximize the correspondence with ground truth (Reinhart et al., 2022). The LANDMATE map is the starting point from which past and future land cover (so called “LUCAS LUC”) maps are generated. To do so, Hoffmann et al. (2023) used the Land-Use Harmonization (LUH2) database, which prescribes the changes in land use consistent with various future scenarios. The final land cover database (herein called LANDMATE for simplicity) is available online:

https://doi.org/10.26050/WDCC/LM_PFT_EUR_v1.1

https://doi.org/10.26050/WDCC/LUC_future_EU_v1.1

The first major task for ASIMLUC-II was to generate analog LANDMATE PFT maps for North America. As a first step, the original cross-walking tables (CWT), which convert ESA-CCI land categories to LANDMATE PFTs were applied to North America. These original CWT were then adjusted to minimize discrepancies with several other databases:

- ESA-based CWT for CLASS with validation over Canada: L. Wang et al. (2019), later refined in L. Wang et al. (2023)
- ESA’s default PFTs, later refined in Harper et al. (2023)
- USGS NLCD 2019 (https://www.mrlc.gov/data/nlcd-2019-land-cover-conus; US only)
- MODIS (EVAL map from FOREST-GRASS experiment of Rechid et al. (2017))
- GLC2000
- USGS GLCC (operational land cover maps at Ouranos)

To compare these databases, a common metric was needed. Since our main goal was to produce land cover maps best suited for CRCM5-CLASS, we projected each database onto the CLASS categories (needleleaf, broadleaf, grass and crops). LANDMATE maps were then compared to the other databases, with L. Wang et al.

[2] LANDMATE comes from “Modelling human LAND surface Modifications and its feedbacks on local and regional climate”.

(2023) and USGS NLCD taken as references over Canada and the U.S., respectively. This lengthy and tedious process was thoroughly documented (see in the annex: /Land Cover Maps/Validation/).

In a nutshell, we adjusted the original LANDMATE CWTs for North America significantly in the Canadian Arctic (less grassland, more bare soil), the U.S. southwest (more bare soil) and the U.S. East Coast (less broadleaf trees, more needleleaf trees). The precise changes in the CWTs are documented in the annex (/Land Cover Maps/Documentation/). The resulting LANDMATE-NA maps are now available online:

https://doi.org/10.26050/WDCC/LM_PFT_NA_v1.1

https://doi.org/10.26050/WDCC/LUC_future_NA_v1.1

To aid visualization of this large dataset, animations of LUC maps were generated for SSP1-2.6 and SSP3-7.0 (see annex: /Land Cover Maps/Visualization/).

4.2.1.1. Validation of LANDMATE and implementation in the Ouranos modeling system

One of the major synergies of ASIMLUC is the improvement of the modeling system at Ouranos. Operational climate simulations at Ouranos use a manually-modified version of an aging land cover product: the USGS Global Land Cover Characterization (https://www.usgs.gov/centers/eros/science/usgs-eros-archive-land-cover-products-global-land-cover-characterization-glcc). The development of LANDMATE allowed a much-needed update of the geophysical fields used in operational simulations.

Before implementing LANDMATE maps in operational simulations, a thorough validation work was carried out (see in-depth analysis in the annex: /Land Cover Maps/LANDMATE-CRCM5 Validation/). In short, important differences are seen in the CLASS vegetation fractions associated with legacy and LANDMATE maps. These are in turn associated with notable differences in climatological mean 2-meter temperature and both its daily minima and maxima. Effects on precipitation are also noted, but it is unclear whether they are statistically significant. Overall, the northern limit of the boreal forest is where the strongest changes are observed, especially during winter and spring. LANDMATE suggests a higher concentration of needleleaf trees in this region, and temperatures (including daily minima and maxima) are accordingly higher than with the legacy land cover maps. It is not clear, however, which one is closer to ground truth. In terms of the CRCM5 bias with respect to ERA5, there is also no clear winner. Switching from legacy to LANDMATE basically means replacing overall cold winter/spring biases by warm winter/spring biases.

Furthermore, there is no guarantee that a land cover map more faithful to ground truth will necessarily reduce biases everywhere. Indeed, the fractional area of each vegetation categories is not the only parameter involved in such biases. Each of the 26 RPN vegetation categories is associated with a host of uncertain parameters, such as albedos, root depth, roughness, etc., which are hard-coded in CRCM5-CLASS. These parameters must also be the subject of inquiry if we are to improve our modeling system. Promising work at the Centre pour l'étude et la simulation du climat à l'échelle régionale (ESCER), for instance, aims to compare the albedo of different land cover maps as interpreted by CRCM-CLASS to satellite albedo products.

The LANDMATE maps were designed for use in regional climate models, hence their 0.1° resolution. The present-day LANDMATE map is based, among other things, on the 300-m resolution ESA-CCI satellite product. It should thus be possible to produce a higher-resolution LANDMATE map for the present day. In fact, such map

exists and is available online at a 0.018° (2 km) resolution for Europe (https://www.wdc-climate.de/ui/entry?acronym=LM_PFT_EUR_v1.1_afm). An equivalent map for North America would be valuable, especially for downscaling experiments using the surface prediction system (SPS). We are currently in contact with Dr. Peter Hoffmann regarding a 2-km resolution LANDMATE map for North America. Note, however, that for years outside of the range covered by ESA-CCI (1992-2015) it will not be possible to attain such high resolutions. Future projections of land cover, in particular, are based on LUH2, which has a coarse 0.25° resolution.

4.2.1.2. Why not simply use the land cover maps from CCCma?

The Canadian Center for Climate Modelling and Analysis (CCCma) hosts several experts of land cover and generated land cover maps of their own, so why reinvent the wheel? Indeed, the initial proposal of ASIMLUC-II was planning on using the CCCma maps, which were kindly shared by Vivek Arora in early 2021. However, it was decided for several reasons to opt for the LANDMATE maps generated in collaboration with the LUCAS team.

First, we realized that using the maps from CCCma, which included the 9 CLASSIC categories, involved a significant loss of information compared with the 16 vegetation LANDMATE categories. CRCM5 ingests vegetation maps in the specific form of 26 “RPN” vegetation categories, which are then aggregated into the 4 CLASS categories. In this process, the information from the biophysical properties of all RPN categories are incorporated independently for each pixel. For instance, if there is a 50-50 split between deciduous shrubs and deciduous broadleaf trees (which are both aggregated as the “broadleaf tree” category of CLASS), there will be a weighted average of shrubs and trees at that pixel. The pixel next to it might have a different ratio of shrubs and trees, and therefore the “broadleaf tree” CLASS category will have different biophysical properties depending on location. Using the 9 CLASSIC categories almost completely homogenizes this rich information, or involves the awkward exercise of first converting the 9 CLASSIC categories into the RPN categories, and then converting them to the 4 CLASS categories. Using the 16 LANDMATE categories, which are straightforwardly converted to RPN categories (see annex: /Land Cover Maps/LANDMATE CWT/), allow to preserve more of this finer-grain information.

Second, it was realized that the CCCma maps did not fully capture the LUC signal. CCCma’s approach is based on Wang et al. (2006), which only uses cropland area change to infer LUC from all land cover categories. This means that any specific forestation efforts, which do not necessarily involve cropland change, would go under the radar. For instance, CCCma LUC maps for SSP1-2.6 have very little tree cover change. It was quickly realized that this was insufficient for a project (ASIMLUC) aimed at assessing the effects of future LUC, such as the ambitious forestation efforts needed to meet the Paris Agreement.

When contacted in the early 2021, CCCma was using GLC2000 as a base for their present-day land cover map. In the meantime, they switched to ESA-CCI as a base, just like for LANDMATE. In the fall of 2024, it was learned from personal communication with Libo Wang at CCCma that there is still ongoing work to improve adjust the ESA-to-CLASS CWTs. Dr. Wang has similarly expressed interest in the LANDMATE dataset. There thus might be point in the near future where CCCma and Ouranos could converge on the land cover dataset used.

4.2.2. Exploratory analysis of LUC effects in Europe

This section assembles all of the unpublished material on ASIMLUC-II simulations over Europe. Section 4.2.2.1 covers the analysis of ERA5-driven runs (blue table in Figure 8). In the spirit of Asselin et al. (2022), LUC effects on the surface balance are decorticated for winter and summer. Section 4.2.2.2 covers all of the ASIMLUC-II ensemble (both blue and green tables in Figure 8). The relative contribution of GHG and LUC to several climatological-mean climatic and hydrological variables of interest is surveyed. This exploratory analysis was key in framing Asselin et al. (2024) around heat waves and the water cycle.

4.2.2.1. LUC effects in ERA5-driven runs

We begin with an analysis of how LUC affect climate in the reanalysis-driven simulations. First, we consider how LUC modify the surface energy balance across the different seasons and scenarios. Then, we explore the physical mechanisms underlying the wintertime and summertime responses and relate them to specific types of LUC.

Surface energy balance

Erreur! Source du renvoi introuvable. summarizes the LUC impacts on the surface energy fluxes and their correlation with temperature, for both scenarios and all seasons. The bubble size represents the average magnitude of the energy fluxes, and its color indicates the correlation of the energy fluxes with the 2-meter temperature. Both the correlation and average flux are calculated over regions of significant LUC (>5%; see Figure 6).

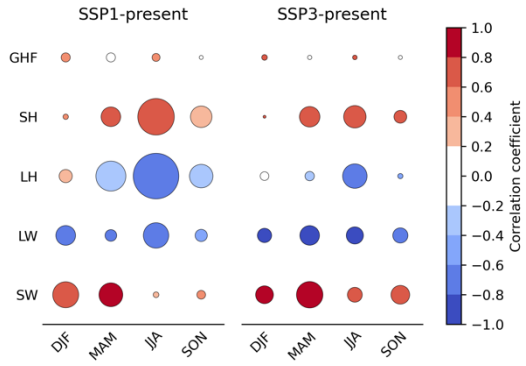

From **Erreur! Source du renvoi introuvable.**, we learn that there is an important seasonal cycle in how LUCs alter the surface energy balance. Changes in shortwave (SW) radiation dominate during winter and spring, whereas latent heat (LH) and sensible heat (SH) fluxes dominate during the warmer months. Longwave (LW) radiation is non-negligible throughout the year, while ground heat fluxes (GHF) never contribute significantly to the changes in the energy balance.

The effect of SW changes on temperature is straightforward: increased SW means more sunlight absorption, hence more energy available to warm the surface (positive correlation). In response, a warmer surface emits more LW radiation, which in effect opposes the warming of the surface. Here the LW signal is predominantly set by the outgoing LW change, which is directly related to the surface temperature as per the Stefan-Boltzmann law (hence the high negative correlation).

Latent heat fluxes represent energy transfers that occur during phase changes of water, primarily through evapotranspiration near the surface. Energy is expended to break hydrogen bonds, diverting it from contributing to surface warming. The result is evaporative cooling (negative correlation with temperature). Sensible heat fluxes represent all convective exchanges that occur without phase changes. During the warmer months, when the surface is typically warmer than the air aloft, these fluxes are positive (positive correlation).

Mechanisms underlying the response

Now that we identified the main components of the energy balance implicated in the climate response to LUC, we will now seek to trace the causal link between LUC and their climate effect. To make the approach more systematic, we computed correlations between each of the LUC and the energy fluxes. In the figures of this section, we show the aggregate vegetation category that is best correlated with the energy flux of interest. Note that LW changes effectively damp surface temperature changes, so despite the high correlation, it provides little insight into the causal chain from LUC to temperature. Therefore, we will stick to SW for the winter, and turbulent fluxes and SW for the summer.

Winter

In both scenarios, there is an overall increase of net shortwave radiation in during winter. This can be traced to changes in albedo, particularly over regions undergoing changes in cropland area (Figure 11). In CLASS, cropland is replaced by bare soil outside of the growing season. Among all vegetation categories, cropland albedo is most sensitive to snow cover: a few centimeters of snow can bury cropland and increase its albedo by up to 0.5 (Figure 12). As a result, albedo is decreased wherever snow covers a region with reduced cropland (Figure 11). The reduction in albedo corresponds to an increase in net shortwave radiation and hence warming of the surface. Correlations between cropland fraction change and 2-m temperature changes reach -0.74 for SSP1 and -0.78 for SSP3. Local warming may reach more than 1°C in some regions in both scenarios.

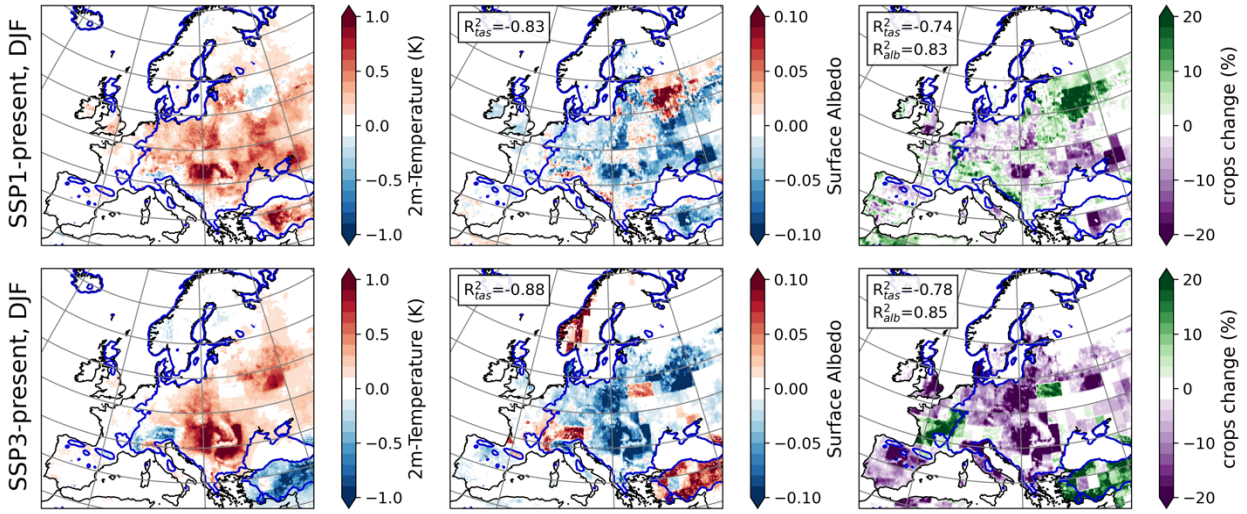

Figure 11 : Near-surface temperature and surface albedo effects of LUC during winter (DJF). The dark blue contour indicates significant (20%) snow cover. Correlations are computed over regions with both significant LUC (>5%) and snow cover. Upper panels: SSP1-present LUC; lower panels: SSP3-present LUC.

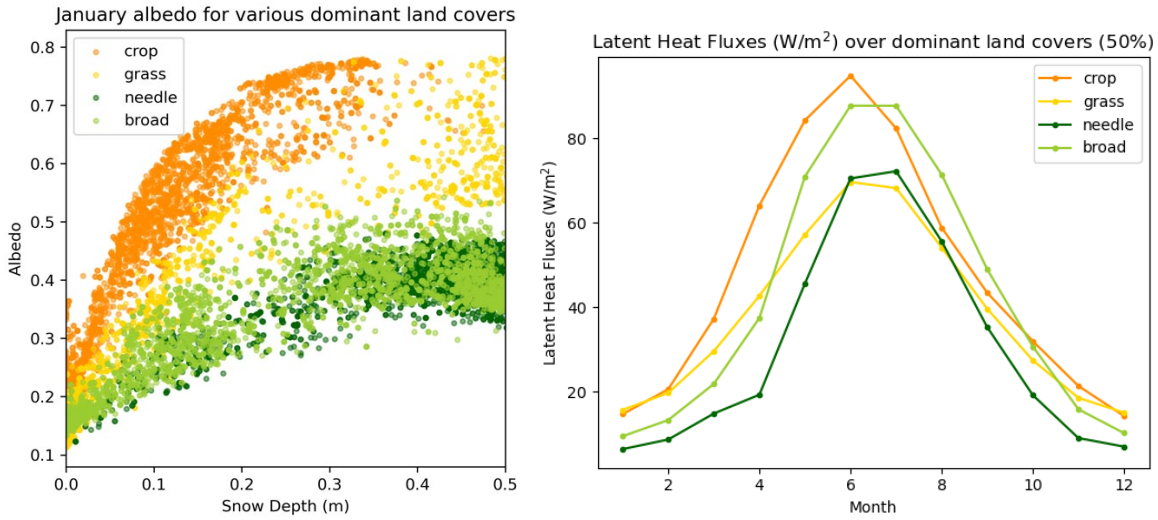

Figure 12: Left : January albedo for dominant CLASS categories (>50% of cover) as a function of snow depth. Averaged over 1986-2015 over present climate and land cover. Right : monthly latent heat fluxes over dominant land covers.

Summer

During summer, the two scenarios diverge significantly, with widespread cooling in SSP1 and widespread warming in SSP3. The main reason for this divergence is a re-partitioning of turbulent heat fluxes by LUC. Since sensible and latent heat fluxes are highly anti-correlated, we consider their difference in Figure 13 and Figure 14.

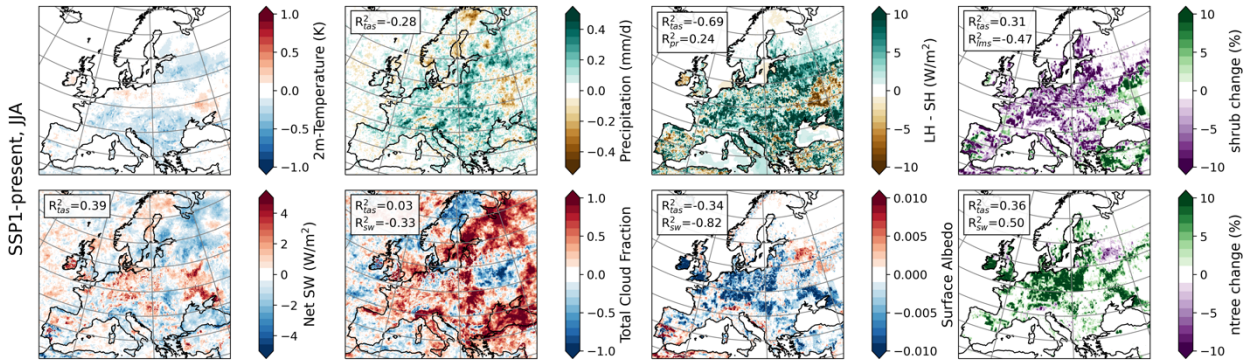

Figure 13: Key variables for the summertime (JJA) response to LUC in SSP1. From top left to bottom right: near-surface temperature, precipitation, latent minus sensible heat fluxes, shrubland change, net shortwave radiation, cloud fraction, surface albedo and needleleaf tree change. Correlations added to the maps are computed between the variable shown in the map and that which appears in the subscript of R. For instance, R_{tas} in the SW panel means that there is a Pearson correlation coefficient of 0.39 between SW and near-surface temperature over regions of significant LUC.

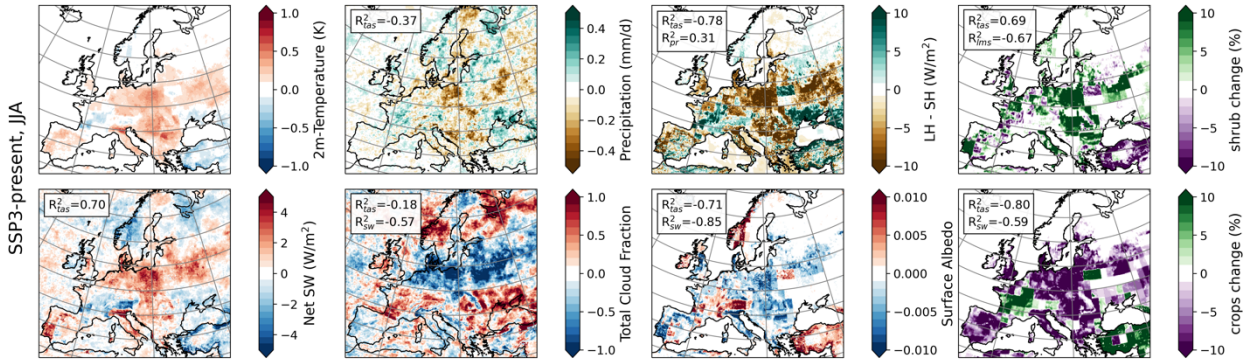

Figure 14 : Key variables for the summertime (JJA) response to LUC in SSP3. From top left to bottom right: near-surface temperature, precipitation, latent minus sensible heat fluxes, shrubland change, net shortwave radiation, cloud fraction, surface albedo and cropland change.

In SSP1, shrub cover decreases at the expanse of trees and evaporative cooling is overall enhanced (Figure 13). This can be traced to increases in stomatal conductance, roughness and leaf-area indices between trees and shrubs categories. The effect of shortwave radiation, dominated by albedo changes, is comparably weaker, but does weaken and sometimes cancel out the cooling from increased evapotranspiration. In particular, needleleaf forestation causes a noticeable reduction in albedo. In fact, in this scenario needleleaf forestation contributes to summertime warming. In SSP3, there is instead an expansion of shrubs over much of Central Europe. This is associated with a sharp decrease in evaporative cooling, which is compounded by a boost in net shortwave radiation (Figure 14). The increase in shortwave comes mostly from albedo (R=-0.85), but also from cloud cover reduction (R=-0.57). The shortwave signal is best correlated with the loss of cropland, which is the most reflective vegetated surface (with grasses).

LUC anticipated in SSP1 and SSP3 also diverge in terms of their effect on precipitation. There is a plausibly a causal link between enhanced (decreased) evapotranspiration and precipitation in SSP1 (SSP3). However, spatial correlation remains low as precipitation generation tends to be non-local. The bottom line is that LUC, mainly the change in transpiration-inhibiting shrubs, causes a widespread summertime warming in SSP3, and a widespread cooling in SSP1. Both scenarios imply a darkening of the surface as cropland is replaced by either trees or shrubs.

4.2.2.2. Relative contributions of LUC and GHG to climatological variables of interest

This section describes the exploratory analysis carried out on the Europe simulation ensemble. The goal of this analysis was to identify variables of interest most influenced by LUC and/or GHG for each scenario. As a first step, we looked at the seasonal and spatial averages of several variables over regions of significant LUC (>5%). For instance, Figure 15 shows how latent heat fluxes are influenced by LUC and GHG in the two scenarios considered. Here we learn that both GHG and LUC drive increased evapotranspiration on average over regions of significant LUC under SSP1-2.6. LUC tend to have more impact than GHG on evapotranspiration and exhibit less inter-member variability. In SSP3, GHG have more impact than LUC on evapotranspiration, and affect winter/spring differently than summer/fall.

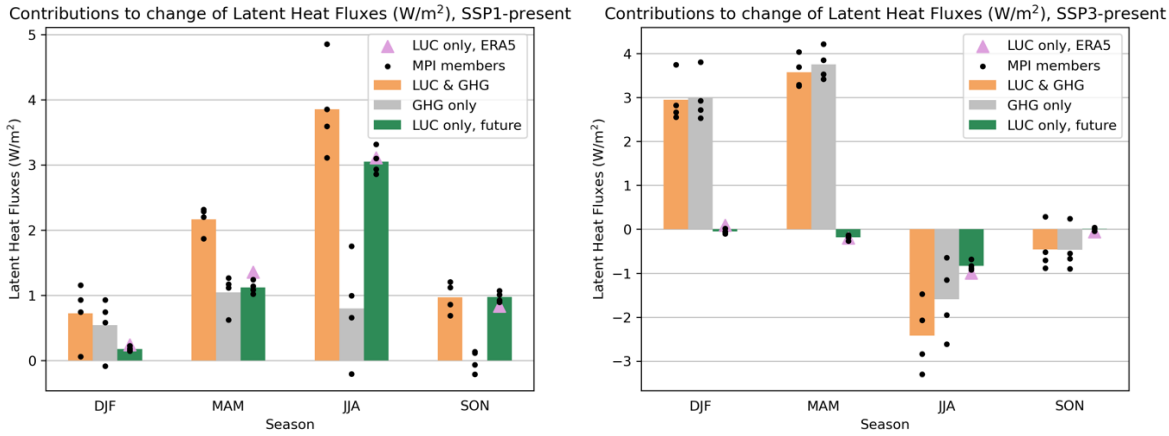

Figure 15: Relative contributions of GHG (grey), LUC (green) and both combined (gold) to latent heat fluxes. Values are averaged over all regions of significant LUC (>5%) in Europe. Small dots represent each of the four MPI-driven ensemble members, and pink triangles is associated with ERA5-driven runs. Left: SSP1-present; right: SSP3-present.

In the annex (Analysis/LUC vs GHG catalog/), all variables of interest are catalogued in a similar fashion. In addition, we show maps of seasonally-averaged contributions from LUC and GHG along with hatching in regions of inter-member disagreement (see Figure 16, for instance).

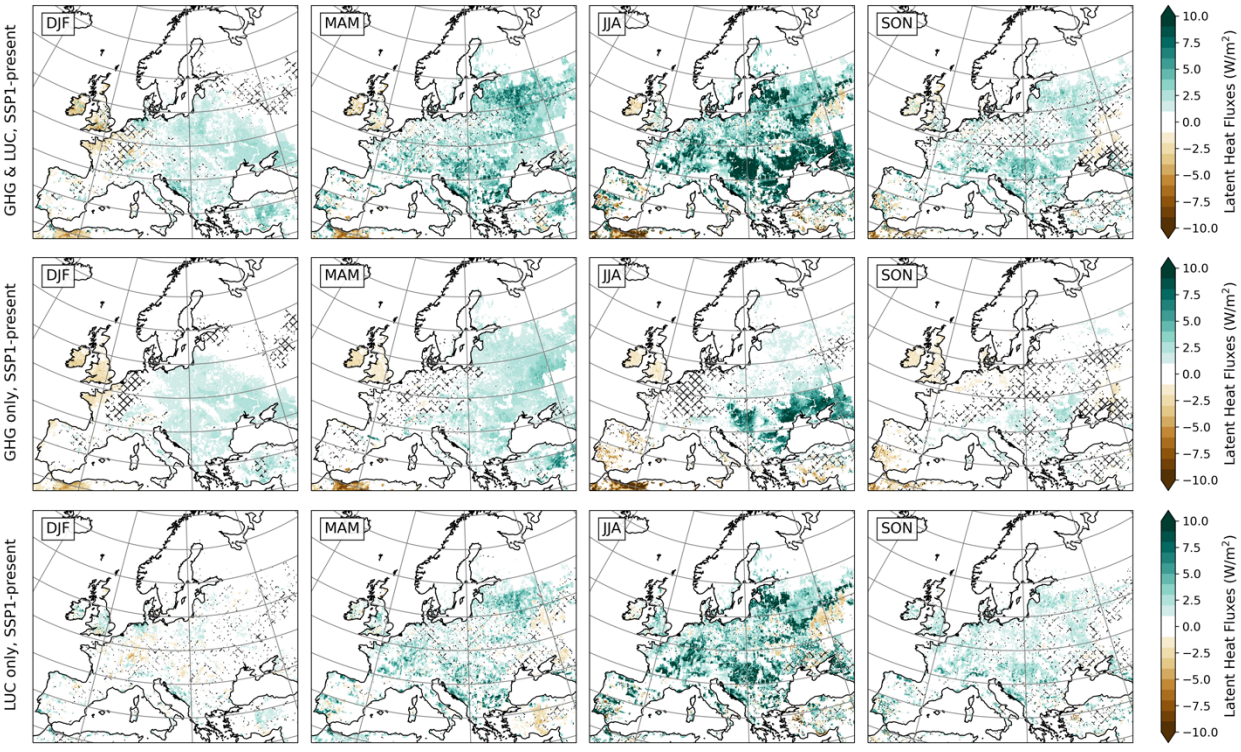

Figure 16: Relative contributions of GHG and LUC on latent heat fluxes under SSP1-2.6. Hatching shows regions of inter-model disagreement (half of the members give a positive delta, the other half a negative delta).

To further synthetize the relative contributions of GHG and LUC to variables of interest, Figure 17 shows matrices of the ratios LUC-induced to GHG-induced delta of a variable for each season and scenario.

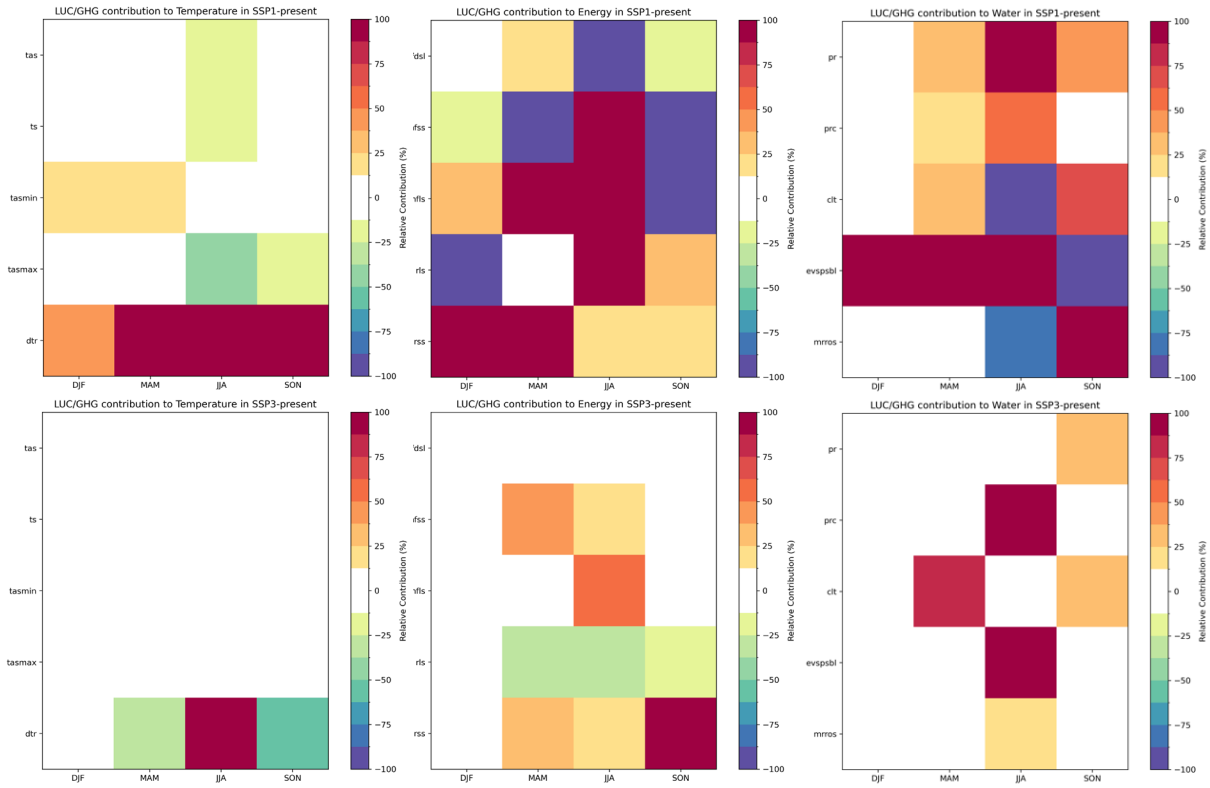

Figure 17: Relative contributions of GHG and LUC on a variety of variables. Upper row: SSP1-2.6. Lower row: SSP3-7.0. From left to right: temperature-related variables, surface energy balance components, moisture-related variables. Red squares mean that LUC-induced change to a given variable have an amplitude at least as great as GHG-induced changes to that same variable, and they share the same sign. Purple means the same, except that the LUC and GHG cause changes of different sign. Each row represents a scenario, and the three matrices assemble, from left to right, variables related to temperature, energy and water.

It is clear from Figure 17 that SSP1 (upper row) is more significantly impacted by LUC than SSP3 (lower row). As anticipated from the analysis of ERA5-driven runs (**Erreur! Source du renvoi introuvable.**), LUC dominate radiative fluxes in the winter and spring, and turbulent fluxes in the summer. We also discover that while LUC exert relatively weak influence on mean temperatures, they have more influence than GHG on the diurnal temperature range (dtr). Furthermore, water fluxes are highly influenced by LUC all year-round, but especially during summer. In Asselin et al. (2024), the subject section 4.2.3, all these dominant LUC effects are weaved into a coherent narrative.

4.2.2.3. Relative contributions of LUC and GHG to extremes

The previous section provides an overview of how LUC and GHG affect the climatology, or long-term average, of several variables of interest. Oftentimes, however, extreme values are more salient to humans. For instance, one might care more about learning that heat waves or floods will be more intense rather than that the average temperature or precipitation will increase with global warming.

Since calculating extremes is much more computationally demanding, we focused on key variables: daily temperature minima and maxima and precipitation. For summertime, we calculated both 95th and 99th percentiles. These two percentiles tend to look similar, except that the higher percentile is more intense and noisier than the former. Here we stick with the 95th percentile, but the 99th percentile maps can be found in the annex (/Analysis/GHG vs LUC Catalog/). The annex also contains extreme cold winter temperatures, which are not shown here.

Figure 18 shows changes in the 95th percentile of summertime temperature and precipitation under SSP1-2.6. The most salient feature is the decrease of extreme daily maximum temperature over much of continental Europe due to large-scale forestation (Asselin et al., 2024). LUC-induced changes in extreme nighttime temperature are less pronounced, with cooling (warming) in regions undergoing broadleaf (needleleaf) forestation. Extreme precipitations are increased over most of continental Europe due to GHG. There seems to be a mild increase of extreme precipitation due to LUC, especially in Central Europe.

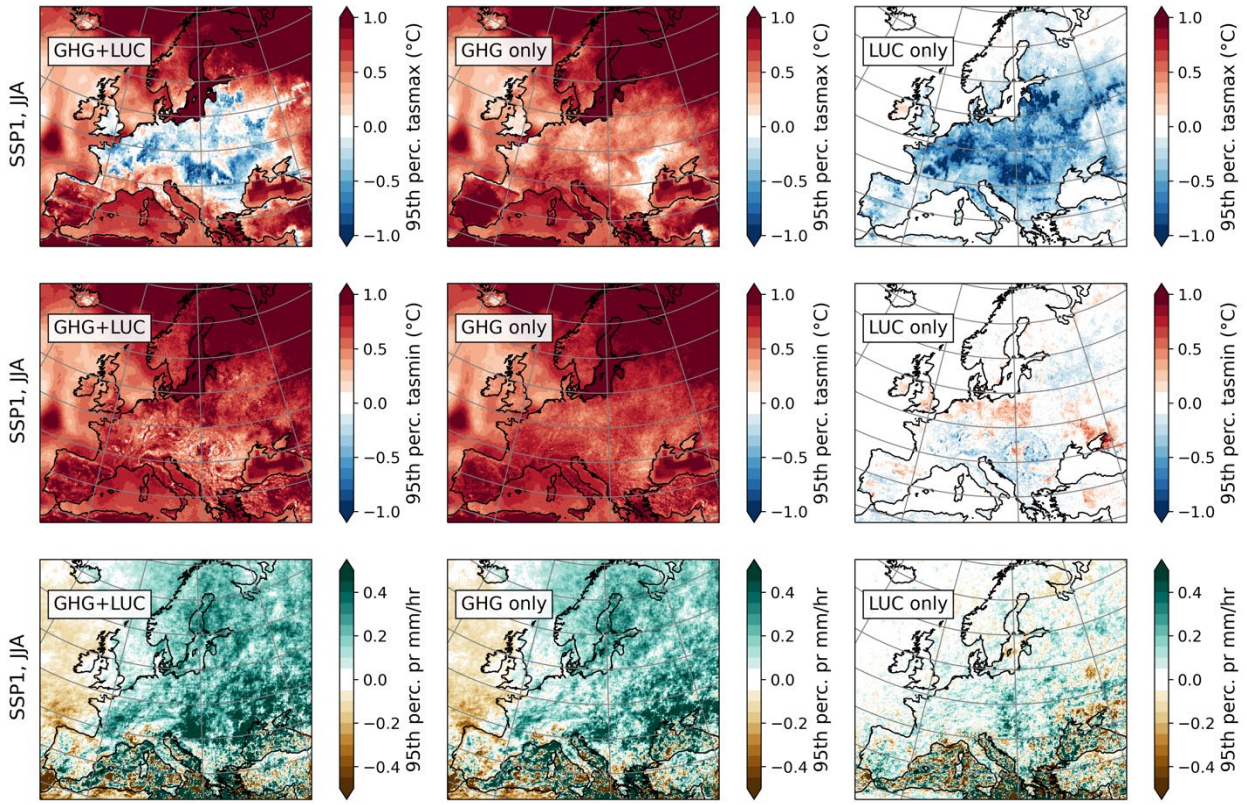

Figure 18: Changes to the 95th percentile of summertime daily minimum and maximum temperatures and precipitation due to GHG and LUC under SSP1-2.6.

Changes in extremes temperature and precipitation look completely different for SSP3-7.0 (Figure 19). Cropland abandonment and shrubification are associated with increased daytime and nighttime temperature extremes. Heat waves are exacerbated by up to 1ºC over Poland. This is a noticeable relative contribution from LUC even if GHG forcing is very strong in this scenario. GHG induce significant boost in extreme precipitation like in SSP1-2.6, but to a greater extent. LUC induce a noisier but definitely negative precipitation extreme signal.

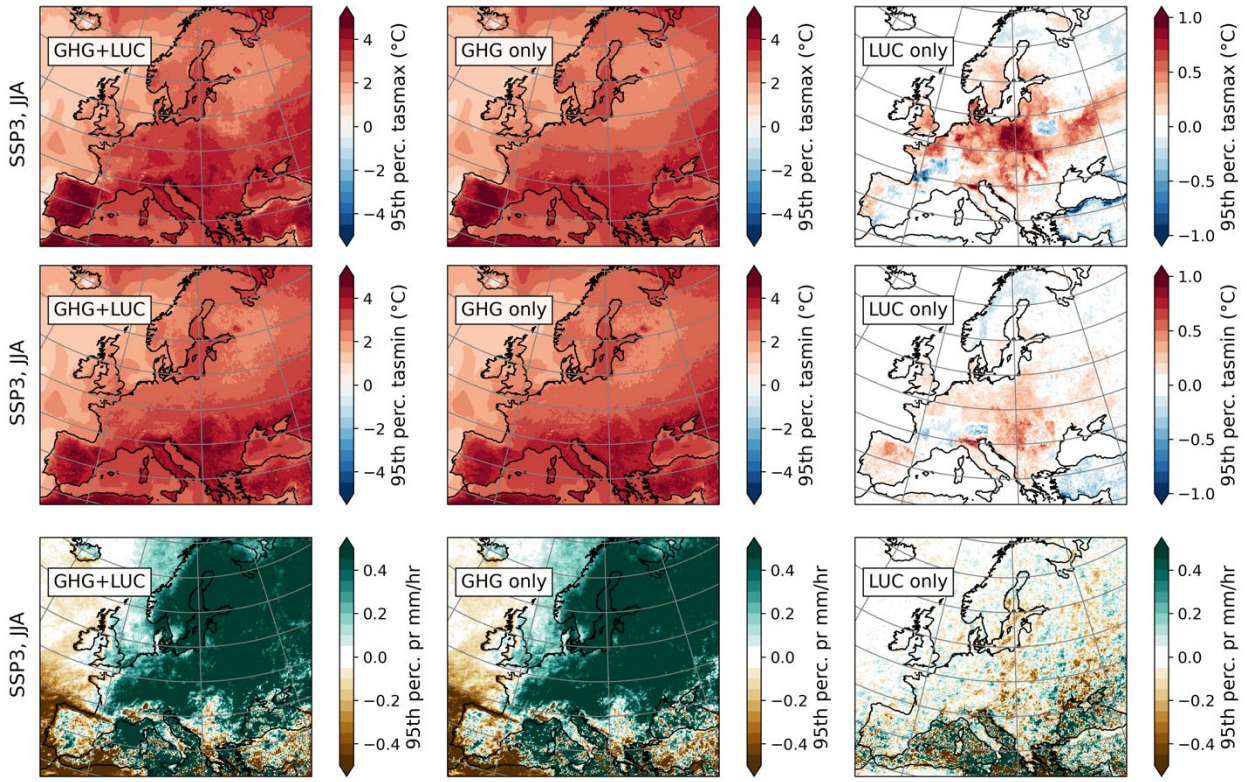

Figure 19 : Changes to the 95th percentile of summertime daily minimum and maximum temperatures and precipitation due to GHG and LUC under SSP3-7.0.

4.2.3. Blue in Green: Forestation in Europe under SSP1-2.6

The main paper describing (a subset of) ASIMLUC-II simulations is "*Blue in green: forestation turns blue water green, mitigating heat at the expense of water availability*", by O. Asselin et al., published in 2024 in *Environmental Research Letters* (see annex: /Publications/Scientific Papers/).

Asselin et al. (2024) shows that ambitious forestation efforts in Europe under SSP1-2.6 could attenuate heat waves in some regions to the extent that they are milder than today by 2100 for half of the population. The process by which this is made possible is summarized in the phrase "blue in green". Planting trees turns blue water (water from rivers, reservoirs, lakes, etc.) into green water (transpiration), which is a jazzy way of saying that trees promote evapotranspiration at the expense of run-off. Energy from the sun is used to evaporate water instead of warming the surface, and hence net cooling results. And while forestation does enhance precipitation on average, this extra water intake cannot fully compensate the loss from evapotranspiration. As a result, soil moisture decreases in some regions, in particular the already-dry southeastern Europe. Put simply, forests mitigate heat waves at the expense of water availability.

Due to the strict word count limit in *Environmental Research Letters*, some interesting details were cut out from the final paper, including former section 3.3, which discusses how the effects of LUC is not just about trees. This is relevant to ASIMLUC-II and therefore the deleted section is included below. To avoid confusion, section and figure numbers from the *Blue in Green* paper are marked with an extra "BG".

4.2.3.1. Deleted section 3.3: Beyond forestation and locality

In the previous sections, we found that 1) of all LUC categories, broadleaf forestation matches patterns of heat mitigation best (section 3.1, BG); and 2) enhanced latent heat is the principal driver of heat mitigation (section 3.2, BG). To complete the causal chain, we now verify that broadleaf forestation is a major driver of latent heat fluxes. Comparing the maps of broadleaf forestation (figure 2, BG) and LUC-induced hot-day ΔLH (figure 4, BG), we find that they share several pronounced fine-scale features such as in France, Germany, Hungary, Russia and the Baltic states. This suggests that broadleaf forestation tends to favor local-scale enhancement of latent heat fluxes.

However, the correlation between broadleaf forestation and hot-day ΔLH is far from perfect (R=-0.43; figure SI-SM3, BG). In fact, patterns of shrub reduction match hot-day ΔLH just as well (R=0.43). While the shrub reduction area is only about half the area of broadleaf tree expansion (figure 2, BG), the evapotranspiration-relevant biophysical properties of shrubs are among the most extreme in our model (table SI-LC1, BG). For instance, shrubs have a minimum stomatal resistance of 855 s/m, which dwarfs all other vegetation categories, whose resistances range between 100 and 250 s/m. Broadleaf trees are among the land categories most favorable to evapotranspiration with their deep roots, low stomatal resistance, and relatively high maximum leaf area index and roughness length. However, these properties are not markedly different from other important categories such as crops, which have even lower stomatal resistance albeit slightly less favorable leaf area index, root depth and roughness. To illustrate this point, the region undergoing broadleaf deforestation at the expense of bioenergy crops in western Russia is actually characterized by a slight *increase* in latent heat fluxes (figure 4, BG) and LUC-induced cooling. Although cropland expansion is on average far less favorable to evapotranspiration than is forestation (R=-0.01 vs R=0.43), other factors clearly play a role. LUC alone cannot fully account for local changes in LH.

In general, we note that correlations between specific LUC categories and the components of hot-day surface energy balance are rather weak, with no combination reaching an absolute value above 0.5 (figure SI-SM3, BG). At least two major sources prevent high correlations. First, there are significant correlations between the different LUC categories (figure SI-SM4, BG). For instance, broadleaf forestation tends to be associated with a loss of shrubs, but not always (R=-0.35), which makes it difficult to disentangle their respective influences on climate variables. Second, it is plausible that LUC may affect the surface energy balance non-locally. For instance, forestation is known to enhance precipitation downwind (Meier et al., 2021). This could cause enhanced evapotranspiration in a region characterized by another category of LUC, blurring the link between forestation and evapotranspiration.

4.2.3.2. Diurnal cycles

Another relevant analysis didn't make the final cut for of Asselin et al. (2024) due to the word count limit: the analysis of energy and temperature diurnal cycles. In the annex (Analysis/LUC vs GHG Catalog/), we select special locations where clear LUC signals occur and analyze how energy and temperature diurnal cycles are modified by LUC, on average and also specifically on hot days. This was a useful exercise to acquire a deeper understanding of the mechanisms involved. Below, we include a section from an earlier version of the paper, which was blended with final section 3.2.

Diurnal Cycle at a Broadleaf Forestation Spot

To illustrate how heat extremes are mitigated by forestation, we analyze the diurnal cycle of energy fluxes and temperature at a specific location experiencing intense broadleaf forestation. This special location, herein called site B, is located at 47°N, 18.5°E. B is near Budapest, but outside of the city center to avoid the artifacts of urban cover. In our present-day land cover dataset, B predominantly consists of cropland (75%) and grasses (18%), with broadleaf trees making up only 3% of the tile's surface see inlet pie chart of Figure 20). At the end of the century, the fraction of broadleaf trees has surged by 38% at the expense of crops and grasses, with negligible changes in the other land categories (inlet graph bar in Figure 20), In response, B experiences a 1.2°C decrease of TX95 due to LUC alone.

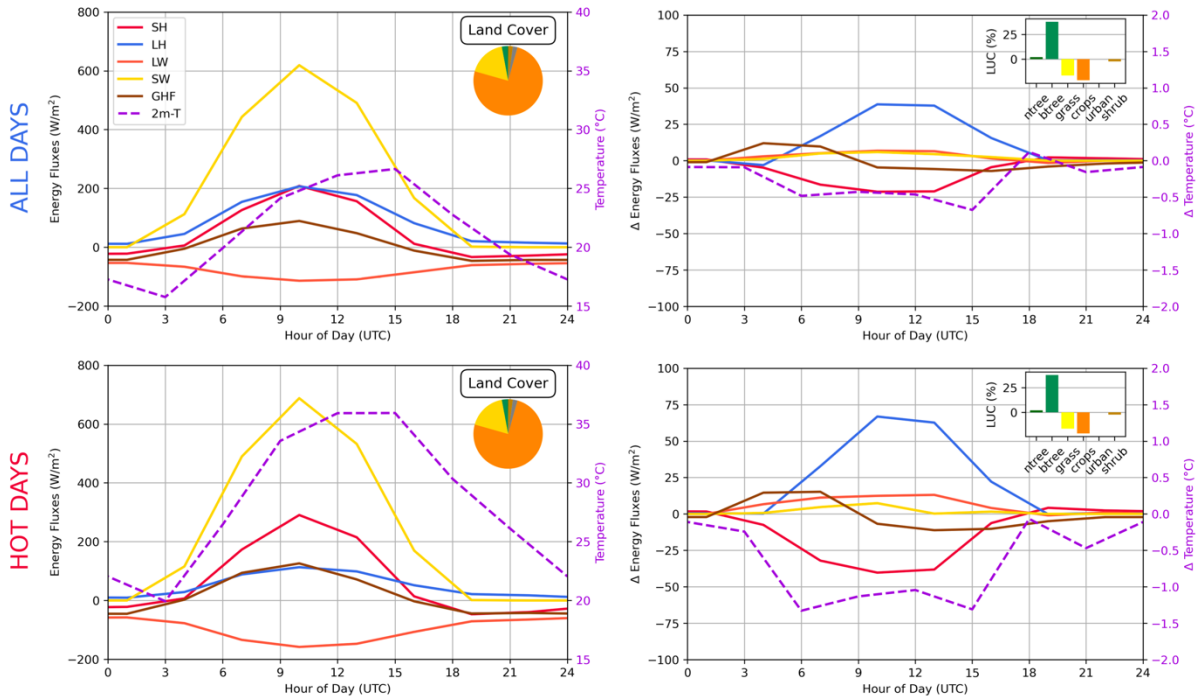

Figure 20: Ensemble-averaged summertime (JJA) diurnal surface energy fluxes and temperature at site B, in the countryside near Budapest. The top row shows the climatology of the region, the bottom row shows the climatology for hot days only, defined as days with maximum temperature exceeding the 95th percentile. The left panels are the absolute fluxes and temperature in present-day climate and with present land cover. The right panels show the change in those quantities due to LUC. The pie charts in the left panels show the present-day land cover fraction: crops (orange), grass (yellow), pale green (broadleaf), shrubs (brown) and urban (grey). The bar graphs included in the right panels show the change between end-of-century and current land cover categories. Energy fluxes are shown in solid lines while temperature is represented by dashed lines.

The Climatology of Regular Days

The top left panel of Figure 20 depicts the daily cycle of energy fluxes and temperature on an average summer day at site B, with present-day land cover and GHG concentrations (G_pL_p). The ensemble average shows a near equipartition between sensible heat (SH) and latent heat (LH) fluxes. Both turbulent fluxes reach their maximum concurrently with the peak of incoming shortwave radiation (SW) and ground heat fluxes (GHF). The 2-meter daily maximum temperature lags by a few hours as the ground heats the lower atmosphere via SH and longwave radiation (LW). On a regular summer day, LH moderates the peak daytime temperature. In effect, LH redirects solar energy away from SH and upwelling LW, which would otherwise result in warming. This redirected energy is instead utilized to break hydrogen bonds, i.e., evaporate water, without direct temperature change. The net result is evaporative cooling.

In our model, the biophysical properties of deciduous broadleaf trees tend to foster high evaporative efficiency of the surface. On an average summer day at site B, forestation is associated with a peak increase of LH by about 35 W/m^2 and a peak reduction of SH by about 25 W/m^2 (upper right panel). In other words, broadleaf forestation promotes evaporative cooling. Importantly, the evaporative boost is largest around midday, because that is when photosynthesis is most active. As a result, daytime temperature and hence the daily maximum temperature are most affected by forestation, with cooling around 0.5°C on a regular day. During night time, photosynthesis does not occur and therefore forestation has little effect on energy fluxes and therefore temperature. In short, broadleaf

forestation at site B favors midday evaporative cooling, and this reduces temperature near the daily maximum, leaving nighttime temperature largely unchanged.

Albedo is often the main property of interest when considering the biophysical effects of forestation, since trees tend to be darker than grasses. This is especially true during winter and springtime, when snow masking by trees can have dominant influence on local temperature (e.g., Asselin et al. (2022)). However, in the case of summertime and more specifically at site B, where broadleaf trees replace crops and grasses, albedo is not so important. In our model, broadleaf trees have a marginally smaller visible albedo (α=0.05) than grasses and crops (α=0.06). The albedo change is detectable in the SW signal, with ΔSW reaching around 5 W/m^2, but this is weak compared to the magnitude of changes in LH and SH. The net LW also increases by about 5 W/m^2 during midday as a result of cooling, which reduces upwelling LW. In sum, the impacts of forestation on the radiative fluxes are dwarfed by the re-partition of the turbulent fluxes.

The Climatology of Hot Days

So far, we have analyzed the diurnal cycle of an average summer day. Let's now investigate conditions on a typical hot summer day. To do so, we compute an average over all summer days for which the maximum daily temperature exceeds the 95th percentile for the given model configuration. The resulting hot-day climatology for site B is shown in the lower left panel of Figure 20. Compared with the all-days climatology (upper left panel), hot days are sunnier (higher peak SW). Nighttime and daytime temperatures are respectively about 5 and 10°C warmer than the climatology. In response, the daily cycles of LW and GHF have magnified amplitudes. Crucially, the partition of turbulent fluxes is heavily shifted towards SH and away from LH, with peak deltas of 100 W/m^2 compared with an average day. Such weak evaporation contributes to an unmitigated peak daily temperature exceeding 35°C on an average hot summer day at site B.

Forestation also provides heat relief on hot days (lower right panel of Figure 20). In fact, the energy flux and temperature responses to forestation are similar to regular days, except with greater amplitude. Compared with its crop-covered analog, forested site B has peak LH about 65 W/m^2 higher and peak SH 40 W/m^2 lower, which is nearly twice the deltas due to forestation on a regular day. This forestation-induced evaporative cooling pulls the daytime temperature about 1.2°C lower, with relatively weak nighttime cooling. In other words, site B analysis reveals that forestation mitigates summertime heat extremes by enhancing latent heat fluxes at the expense of sensible heat fluxes. Such evaporative cooling is particularly potent during hot days.

4.2.4. LUC effects on the water cycle in North America

In collaboration with Prof. Alexis Berg (Université de Montréal), a Masters project was proposed on the impacts of LUC on the water cycle in North America using ASIMLUC-II simulations. Masters' candidate Juliette Goulet started working on the project in late April 2024, and her work is still ongoing at the time of writing. A scientific paper summarizing these findings is expected in 2025. In the meantime, we provide a summary of preliminary results below.

4.2.4.1. Biophysical effects of LUC under SSP1-2.6

Figure 21 shows how LUC under SSP1-2.6 affects climate and hydrology in North America. Forestation of the Canadian prairies and U.S. Midwest reduces albedo, especially during winter and spring when snow coverage is involved, leading to a significant warming of about 2C. In contrast, deforestation in the northeast and southeast of the U.S. and is accompanied with cooling. There is also decreased albedo and cooling associated with a grass-to-crop patch in the center of the U.S, probably because bare soil (cropland during the cold season) is most easily buried in snow. In sum, an albedo-driven temperature response dominates winter and spring, when and where evapotranspiration is weak and the presence snow amplifies albedo changes.

During the summer, there is no strong temperature signal in the strongly forested prairies and Midwest. The transition between (mostly) broadleaf trees and crops (but also a loss of grasses and gain of needleleaf trees) causes weak and canceling effects on albedo and evapotranspiration. The most significant temperature response is a cooling of the southeast U.S. driven by increased evapotranspiration. It is interesting that evapotranspiration increases almost everywhere despite the patchwork of various land transitions. In general, one finds that crops and broadleaf trees tend to be most favorable to evapotranspiration, while shrubs and grasses tend to drive decreased evapotranspiration (which seems consistent with the analysis of dominant land covers in Europe shown in Figure 12).

LUC also drives increased precipitation recycling in the eastern U.S., broadly over regions of increased precipitation. The signal is strongest during summer, when vegetation is most active. The resulting run-off signal is complex and patchy, with clear reductions along the south and east coasts of the US, where evapotranspiration increases but precipitation decreases. The next step will be to perform a statistical test to assess how much of the water flux signals can be ascribed to LUC-induced dynamics versus internal variability.

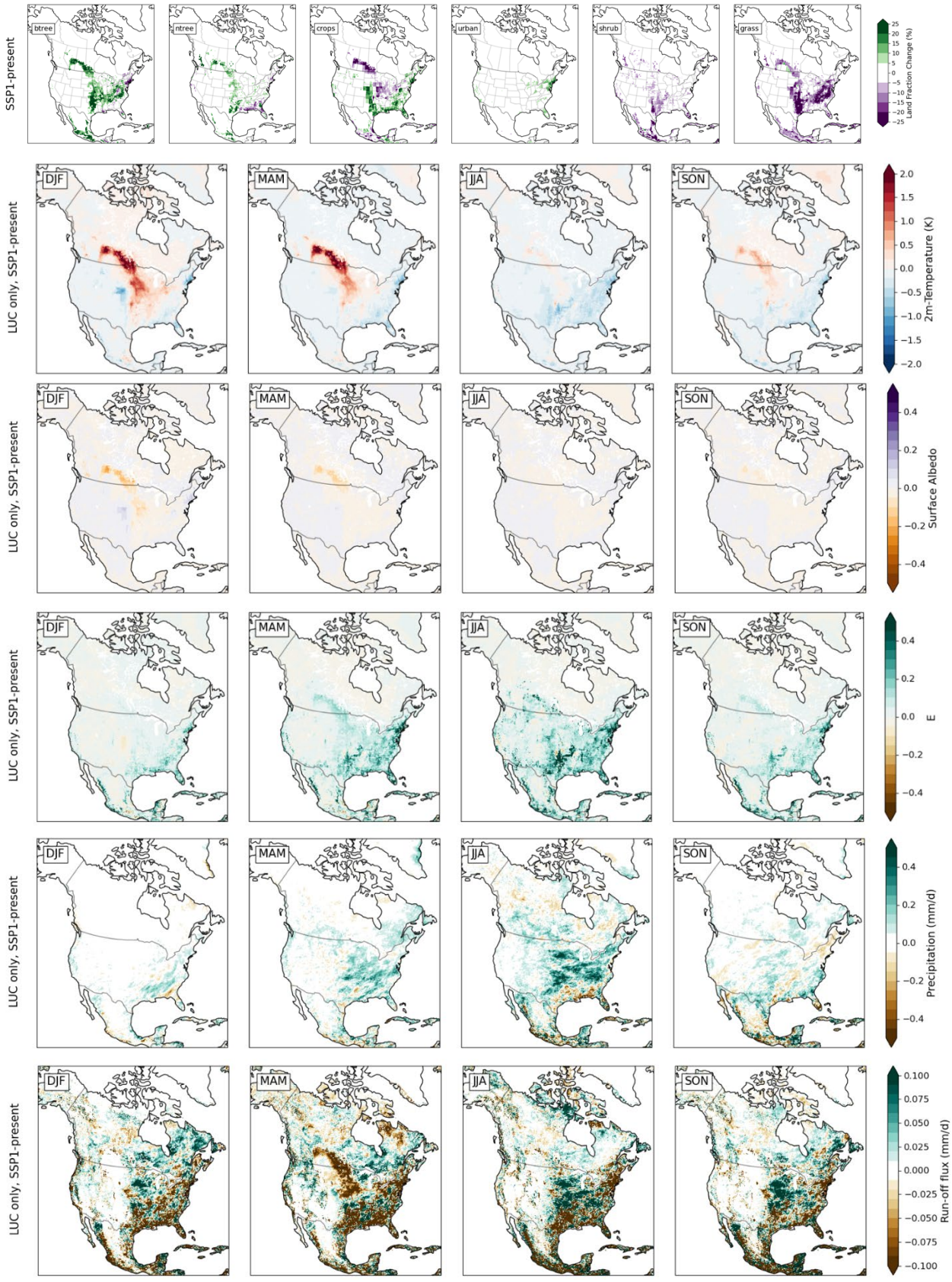

Figure 21: LUC-induced changes for a few ensemble-averaged variables under SSP1-2.6.

4.2.4.2. Biophysical effects of LUC under SSP3-7.0

The LUC signal under SSP3-7.0 is characterized by a severe transition from trees to crops on the East Coast of the US and southwest of Canada (Figure 22). During the snow season, albedo increases and cooling ensues in those regions. A crop-to-grass patch in the center north of the US is associated with decreased albedo and warming, probably due to snow burial of cropland. The evapotranspiration signal is somewhat puzzling. There is significantly more evapotranspiration along the East Coast for all seasons, where crops now replaced trees, even during winter when crops are expected to be dormant[3]. It is plausible that this evapotranspiration boost contributes to the cooling response in the southern East Coast in winter and spring. During summertime, we also see clear evidence of evaporative cooling from deforestation both in the southwest of Canada and along the east coast of the continent. One of the next steps will be to investigate which biophysical properties are responsible for this.

The precipitation recycling signal is not as clear under SSP3-7.0, with a preponderance of noisy patches in most regions and during most seasons. That said, there might be a significant signal for increased precipitation over the southeast during spring and over the Midwest during summer and fall, but this should be verified with an appropriate statistical test. Due to a robust evapotranspiration increase superimposed with more noisy precipitation, the run-off signal exhibits a clear decrease over the east coast.

[3] In CLASS, crops are planted at dates depending on their latitude and hemisphere. In North America, the Julian days corresponding to the plantation of crops is given by bands of 10 degrees:

{0, 0, 75, 106, 136, 167, 167, 167, 167}

This means that crops below 20°N are perennial, and plantation dates between 20°N and 60°N vary from March 15th to June 15th.

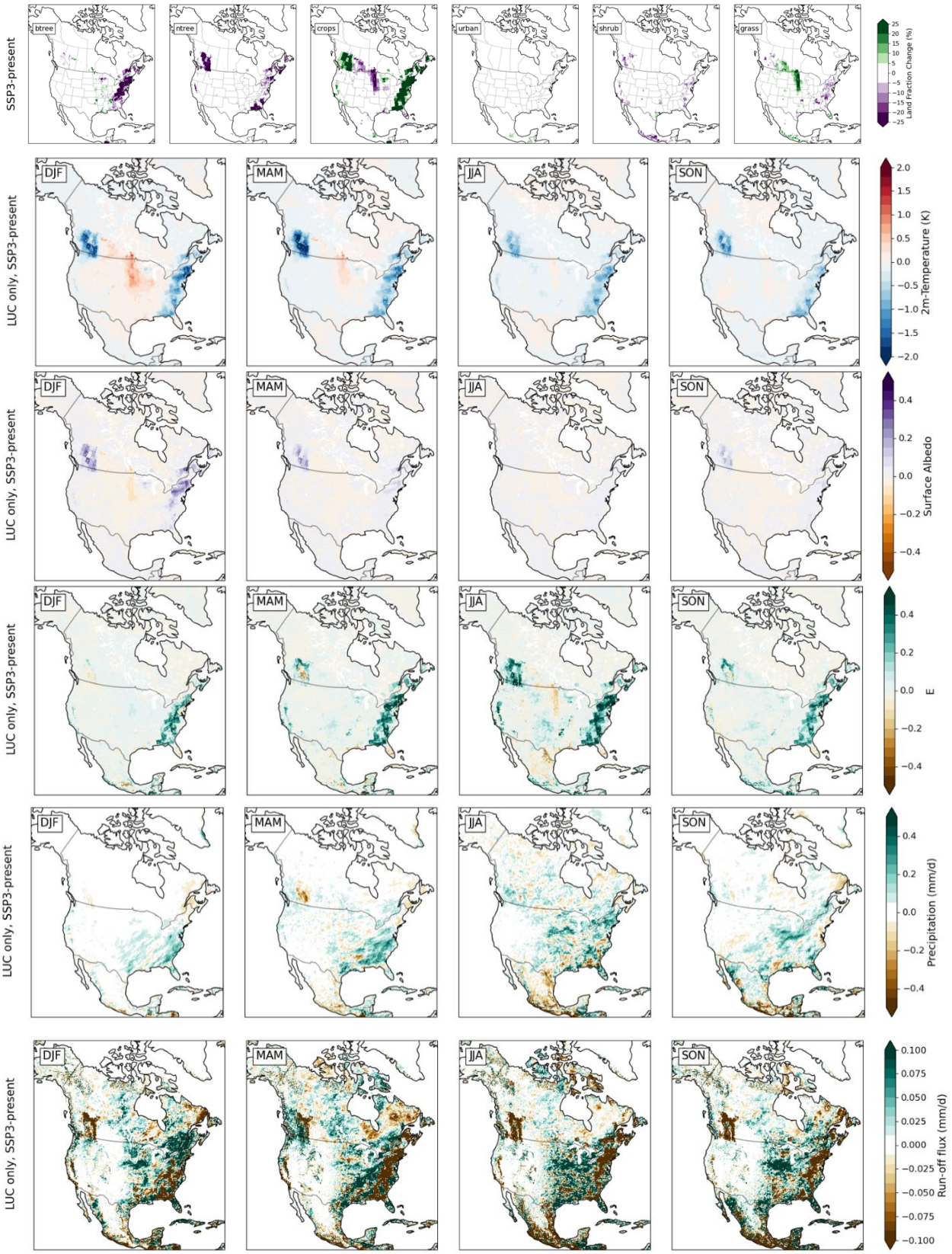

Figure 22: LUC-induced changes to a few ensemble-averaged variables under SSP3-7.0.

4.2.4.3. Beyond FOREST-GRASS

So far, this work allowed to highlight interesting differences between realistic LUC scenarios and the idealized FOREST-GRASS experiments. In particular, the North America future scenarios feature large changes in cropland area, which are excluded in the FOREST-GRASS experiment. Perhaps surprisingly, cropland in CRCM5-CLASS tends to favor more evapotranspiration than even broadleaf forests. This was also seen, albeit at smaller scale, in the Europe simulation under SSP1-2.6 (see southwest Russia in figure 6 of Asselin et al. (2024)). Crops have a notably small stomatal resistance in CRCM5-CLASS, and this may explain deforestation for cropland expansion is associated with increased evapotranspiration (Figure 23).

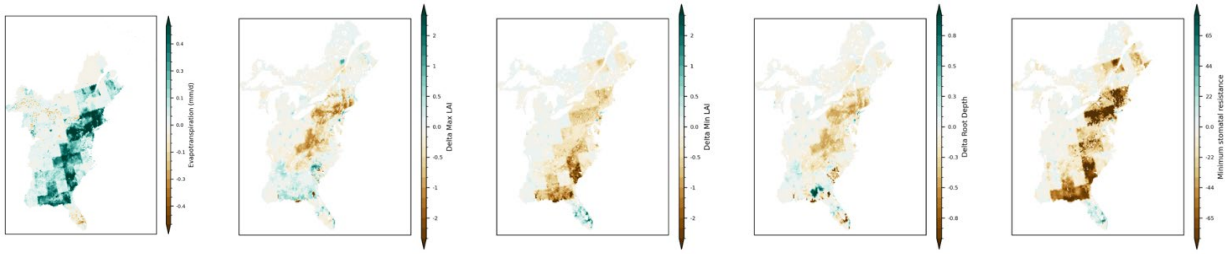

Figure 23 : Changes in evapotranspiration and key related biophysical properties due to LUC under SSP3-7.0 on the eastern coast of North America. From left to right: changes in evapotranspiration, maximum and minimum leaf area index (LAI), root depth and minimum stomatal resistance.

A supplementary factor which may explain why crops tend to favor more evapotranspiration than trees on the east coast has to do with topography. Roughness reduction related to extreme deforestation in SSP3-7.0 is mostly neglected because it occurs in mountainous regions, as CLASS only takes into account the “effective roughness”, i.e., the larger between orographic and vegetation roughness (see further discussion in section 4.3.3.1). If the effects of roughness are neglected, it is plausible that the lower minimum stomatal resistance of crops is the determining factor setting the ease of transpiration.

4.3. LUC AND WINDS

Wind is another key climatic variable strongly impacted by LUC. For instance, forestation can radically alter surface roughness, which is a crucial factor determining the wind profile above the surface. The evolution of near-surface wind has major implications in wide range of sectors from infrastructure to wind energy production. We begin by summarizing a co-authored paper that explores the impacts of extreme LUC on wind energy in Europe (section 4.3.1). Although this paper did not directly utilize CRCM5-CLASS, it brought important lessons for future projects on wind at Ouranos. Subsequently, we provide an overview of key results from the extensive analysis of both phases of ASIMLUC, assessing the impacts of various LUC scenarios on wind over North America (section 4.3.2). This analysis highlighted some important limitations concerning winds in mountainous regions and in very stable atmospheric regimes (section 4.3.3). In section 4.3.4, we discuss the various lessons learned from analyzing ASIMLUC winds and whether we recommend pursuing this analysis further.

4.3.1. Extreme LUC effects on wind energy in Europe

The LUCAS team was contacted by Jan Wohland to access wind data from the FOREST-GRASS multi-model ensemble. Unfortunately, wind data from several models (including CRCM5-CLASS) were not retained because they were only available on pressure levels. For wind energy applications, it is preferable to have wind data on constant-height levels. Nevertheless, yours truly contributed to the resulting paper, "*Extrapolation is not enough: Impacts of extreme land-use change on wind profiles and wind energy according to regional climate models*" by Jan Wohland et al., published in the scientific journal *Earth Systems Dynamics* (see annex: /Publications/Scientific Papers/).

Wohland et al. (2024) explore the impacts of extreme deforestation on wind speeds and wind energy potential. The study emphasizes the limitations of extrapolating near-surface winds to higher altitudes using traditional methods and highlights the importance of using vertically resolved, sub-daily output from regional climate models for accurate wind energy assessments.

Afforestation is shown to significantly reduce wind speeds up to 300 meters above the ground across Europe, with reductions exceeding 1 m/s in many locations. These changes are crucial for wind energy calculations as they substantially affect the wind energy capacity factors. The study critiques the standard practice of using extrapolation methods, which fail to capture essential spatiotemporal details and might lead to significant errors in estimating wind energy potential. Extrapolation methods, although approximating long-term means well, do not account for variations in daily cycles and other temporal aspects critical for understanding wind energy dynamics.

4.3.2. Exploratory analysis of wind in North America

4.3.2.1. Topography, roughness and wind

The analysis of wind data spanned both phases of ASIMLUC. Figure 24 illustrates the range of roughness and wind speed changes covered by the three main LUC scenarios considered: FOREST-GRASS (complete afforestation), SSP1-present (mostly forestation) and SSP3-present (mostly deforestation). Despite the wide range of LUC transitions included, we find that climatological wind speed changes obey a relatively robust linear relationship with roughness, at least for changes in roughness lengths up to about 1 m. That is, almost all grid points fall onto the two quadrants where changes in roughness and wind are of opposite sign. This suggests that roughness is the main biophysical property involved in driving the impacts of LUC on winds.

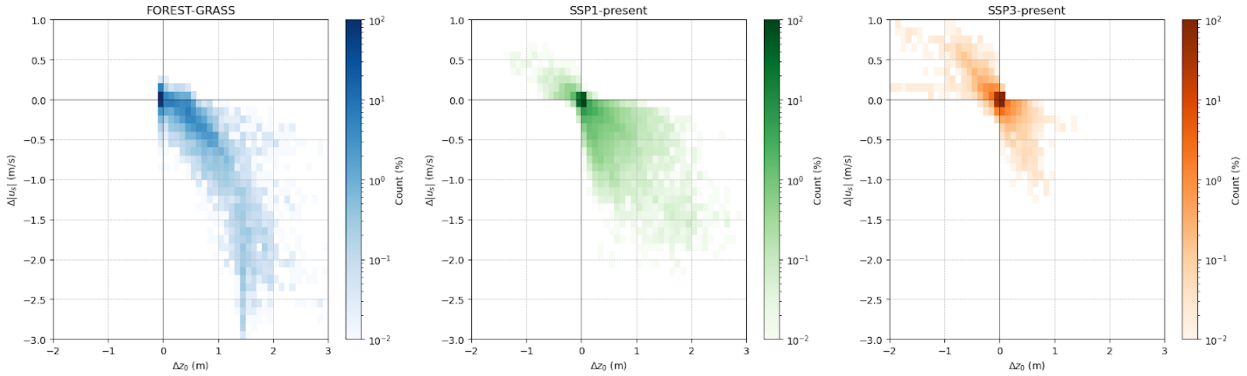

Figure 24: Two-dimensional binned distribution of roughness and climatological surface wind speed changes for each of the three scenarios considered. Water bodies are not included.

However, the value of this roughness length used by CRCM5-CLASS is not entirely set by vegetation height. As we learned in the course of this analysis, CLASS uses an 'effective roughness' to take into account some of the combined effects of sub-grid topography and vegetation. In particular, only the largest of orographic and vegetation roughness is considered:

$$z_{0,eff} = \max(z_{0,oro}, z_{0,veg})$$

As a consequence, roughness changes associated with LUC may be ignored in some mountainous regions. This is what we see in Figure 25, which shows how topographic roughness relates to LUC and associated roughness and near-surface wind change. In FOREST-GRASS (upper row), despite near-complete and uniform afforestation of the continent, roughness changes are far from uniform. There is almost no detectable change in roughness in the mountainous western part of continent, with topographic roughness reaching in excess of 2 meters over wide swaths of the Rockies. The Appalachians cause another prominent gap in the roughness change map. The resulting roughness change map matches the climatological near-surface wind change closely, with wind slowing down in the flatter regions of the continent center and on the eastern shoreline.

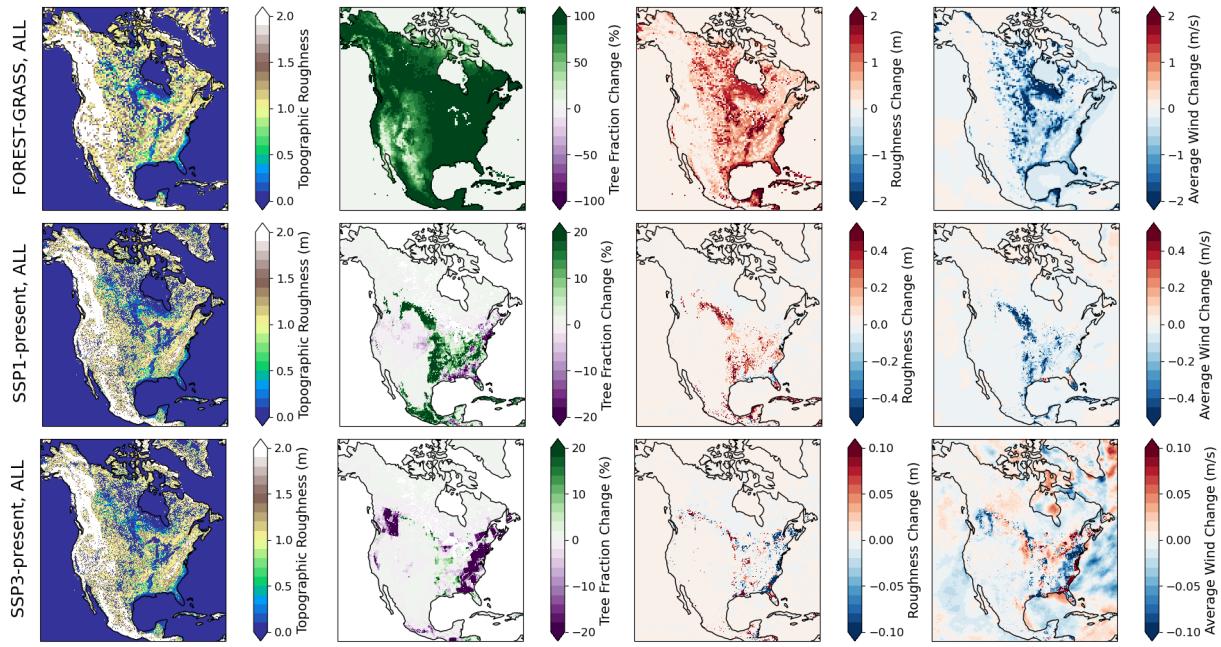

Figure 25: Topographic roughness versus changes in tree fraction, roughness and climatological near-surface wind for LUC scenarios FOREST-GRASS (upper row), SSP1-present (middle row) and SSP3-present (lower row).

Under SSP1-2.6 (middle row), much of the afforestation occurs in the flat Great Plains, such that LUC translate into significant changes of roughness and hence wind. Under SSP3-7.0 (lower row), massive deforestation actually occurs mostly in the southwest of Canada and on the East Coast, where the Rockies and Appalachians respectively reign supreme. As such, roughness and wind changes are far weaker in this scenario despite the strong LUC signal. Minimal roughness change in the Appalachian region may help explain why stomatal resistance exerts such strong control on evapotranspiration, as discussed in section 4.2.4.3.

4.3.2.2. ASIMLUC-I: LUC effects on wind at the surface and aloft

Figure 26 shows roughness and its relationship to near-surface winter winds, both average and at high percentiles, in the FOREST-GRASS experiment (ASIMLUC-I). In general, higher roughness is associated with calmer winds. Water bodies are characterized by low roughness and hence strong winds. Similarly, clearing forests for grassland reduces roughness hence increases wind speed. The stronger the wind, the stronger the influence: as one moves to higher percentiles, the absolute change in wind speed due to extreme LUC becomes greater.

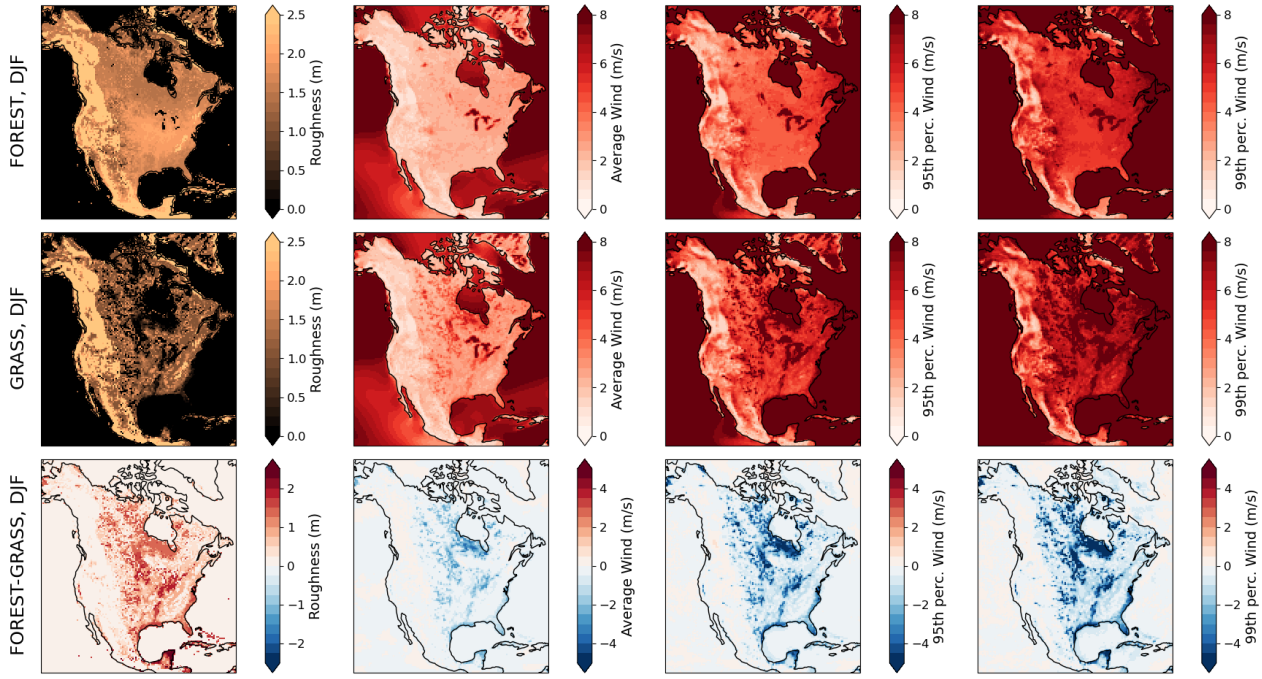

Figure 26 : Roughness, average wind and its 95th and 99th percentile for FOREST, GRASS and their difference. Maps are for wintertime (DJF).

Figure 27 displays how the whole wind speed distribution shifts between FOREST and GRASS experiments at two locations undergoing large roughness changes. In these locations, the 95th percentile wind is nearly slashed in half between FOREST and GRASS simulations.

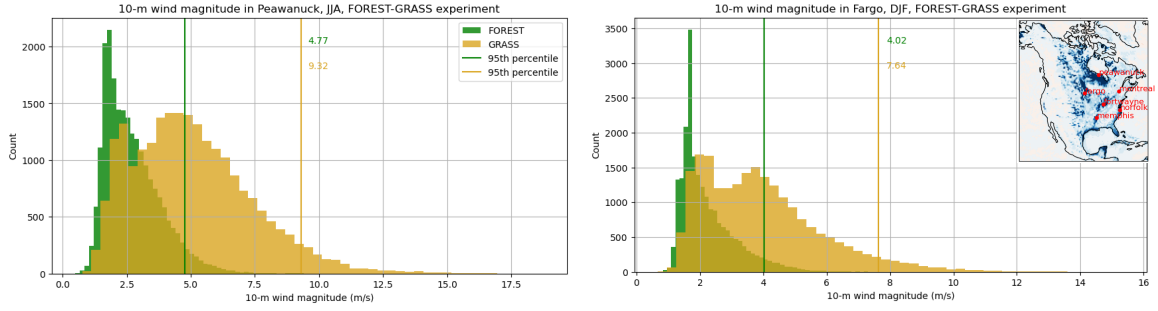

Figure 27: Wind speed distributions at two specific locations for FOREST (green) and GRASS (gold) simulations. Left: Peawanuck, in Northern Ontario; right: Fargo, bordering North Dakota and Minnesota in the US Midwest. Vertical lines depict the 95th wind speed percentiles.

So far, we only looked at near-surface (10-meter) winds, but the influence of extreme LUC extends far higher aloft (see Figure 28). Average and high-percentile winds are significantly affected over the whole atmospheric column, especially up to around 800 hPa, or typically around 1-2 km above the ground (see color distributions on the right-hand axis of the figure). We also looked into the effects of extreme LUC on the location of the Jet Stream but found little signal, potentially because spectral nudging is too strong at these levels.

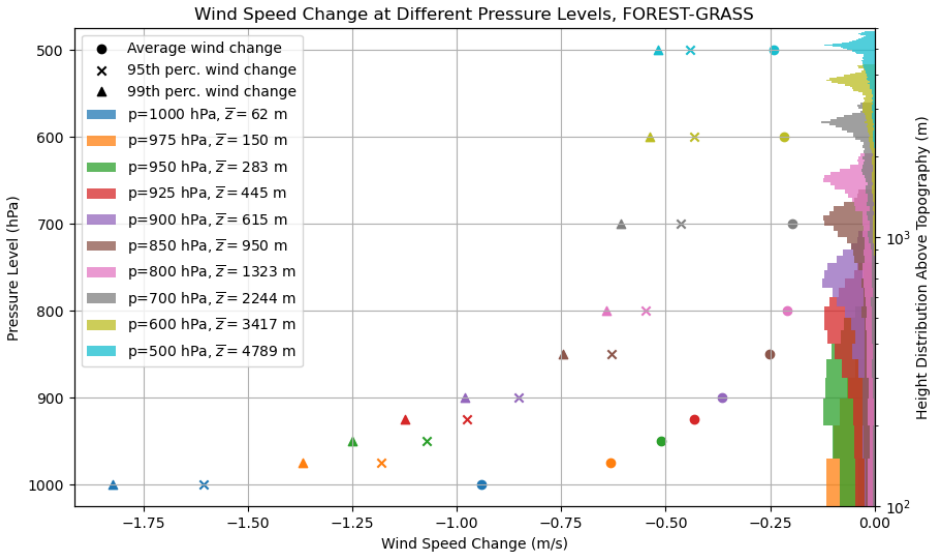

Figure 28: Change in the wind profile in FOREST-GRASS. Points, crosses and triangles represent average, 95th and 99th percentile wind speeds at different pressure levels. The distribution of heights above topography is depicted as bar graphs on the right axis. Each color represents a different pressure level.

Another important feature highlighted by Figure 28 is the wide range of height associated with each pressure level, on which the model output is interpolated. One thus has to be cautious when interpreting LUC effects on the wind profile. Even for relatively low pressure levels, some regions may be below ground (Figure 29).

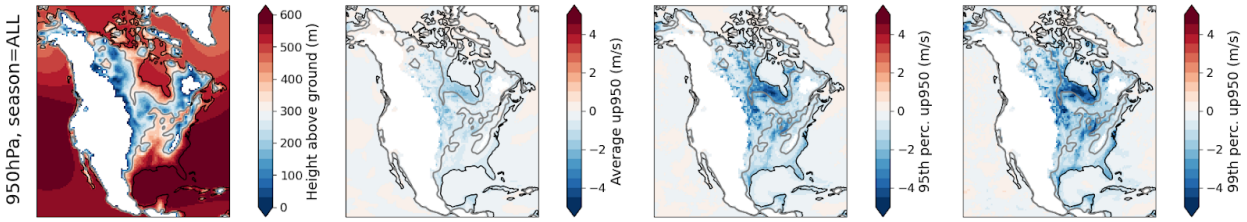

Figure 29 : Left to right: height of the 950 hPa isobar above topography, average, 95th and 99th percentile of wind modulus at 950hPa. Masked values are below ground. Contour at 300 m above ground.

4.3.2.3. ASIMLUC-II: Relative contributions of LUC and GHG on near-surface wind

Figure 30 shows how LUC and GHG affect ensemble-averaged near-surface wind speeds. Under SSP1-2.6, large-scale forestation of the Eastern U.S. and Canadian Prairies has a direct effect on local wind speed, with reductions of more than 10% of the climatological wind. GHG forcing induces a wind slowdown of a few percent over the Pacific and western portion of the continent. This may be due to a reduction in the equator-to-pole gradient and consequent weakening of the westerly jet (Wohland, 2022) or increased occurrence of blocking (personal communication with Sara Pryor). There is also noticeable increase of wind speed in the Beaufort Sea and Canadian Archipelago, which may be linked to reduced sea ice coverage and concurrent decreased in roughness and atmospheric stability (Mioduszewski et al. (2018); Zapponini & Goessling (2024)).

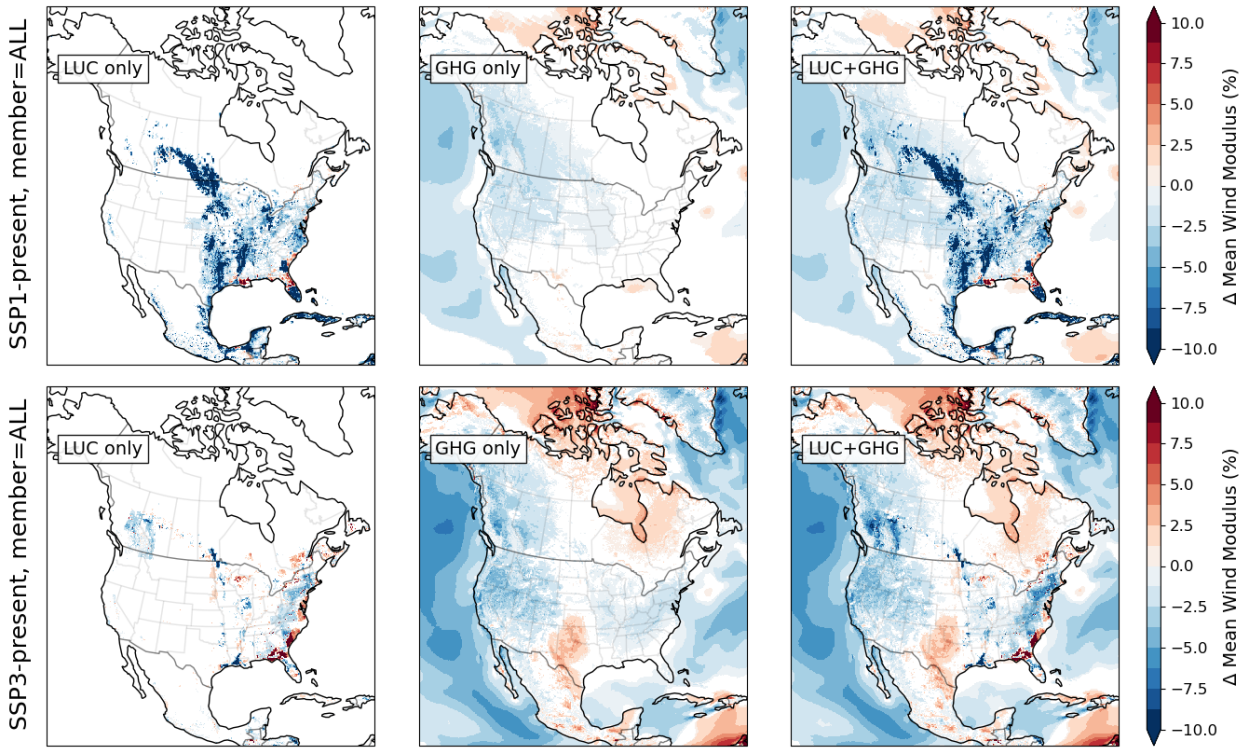

Figure 30: Effects of LUC and GHG on ensemble-averaged climatological wind speed in ASIMLUC-II. Changes are normalized by the control climatology. Statistically insignificant pixels are masked following a two-sided Wilcoxon rank-sum test. The p-values obtained were submitted to a Benjamini-Hochberg correction with a false discovery rate of 0.05.

Under SSP3-7.0, LUC have relatively weak effect on winds, despite widespread deforestation. There are nevertheless small patches that are significantly affected by forestation (Manitoba) and deforestation (along the U.S. east shore). These areas are relatively flat, and therefore LUC is accompanied by strong changes in roughness. Interestingly, the main deforestation regions (Western Canada and Appalachians) show a mild weakening of near-surface winds. This is independent of roughness, which is left essentially unchanged in these mountainous regions. The significant cooling brought by cropland, also seen in western Russian cropland expansion (Asselin et al., 2024), may be increasing atmospheric stability and therefore slightly reduce wind speed.

Strong GHG forcing under SSP3-7.0 induces similar patterns of wind change, but with higher amplitude than in SSP1- 2.6. New significant patterns emerge, such as a wind increase over Texas as well as slowdown over the mid-latitude Atlantic. The Arctic slowdown now extends in-land around the Hudson Bay.

Analysis of these GHG-induced changes in wind could be of great scientific and practical interest, in particular the Texas feature. This is not the first time a significant change in wind due to climate change is simulated in this region, which is a major hot-spot for wind energy production. In fact, a similar wind increase appears in WRF simulations forced by MPI-ESM-LR (but not MPAS) in Pryor et al. (2020), and in a four-member ensemble of different RCM/GCM in Johnson & Erhardt (2016) (see also Pryor & Barthelmie (2011)).

That said, the ASIMLUC-II dataset is not necessarily the best suited for such a study. While it comprises 4 members and two GHG scenarios, downscaling is only done with a single GCM. A better dataset for analyzing the Texas hot-spot could be the CMIP6-CRCM5 operational ensemble by Ouranos, which contains 4 GCMs, 4 GHG scenarios and 5 members for one of the GCMs.

4.3.3. Limitations

The exploratory analysis of winds revealed a few limitations of CRCM5-CLASS of interest for this project. In this section, we identify two potential limitations of interest—winds in mountainous regions (section 4.3.3.1) and winds at low speed (section 4.3.3.2)—and what one might do about it.

4.3.3.1. Effective roughness

Section 4.3.2.1 shows how winds are influenced by roughness, which in turn depends both on LUC and topography. Is it realistic to assume, as CLASS does default, that the roughness of vegetation is negligible when the roughness associated with sub-grid topography is greater? While this feature made wind experts such as Sara Pryor and Andrea Hahmann frown, personal communication with Joe Metlon from September 2024 — a lead voice in the development of CLASS(IC) — would suggest that this is not as unreasonable as it seems.

On a different occasion, we discussed this topic with surface modeling expert Stéphane Bélair from ECCC. In particular, the new version of the climate model, CRCM6-GEM5, includes a turbulent orographic form drag (TOFD) by default. In principle, when this is switched on there is no need for an orographic roughness, and therefore the effective roughness condition is bypassed[4]. According to Dr. Bélair, the use of effective roughness is not satisfactory to surface 'purists' from a theoretical point of view, and therefore the use of TOFD is particularly beneficial if only for getting rid of orographic roughness.

In sum, one gets the feeling that while effective roughness is not unreasonable (and definitely not there by mistake), it would be preferable to adopt more modern ways of dealing with sub-grid orography. In a sense, it is a bit of a bummer that LUC-induced roughness changes are ignored in a LUC study, but at the same time this might provide an opportunity to study the effects of roughness in isolation.

[4] Exploratory analysis of winds in CRCM6-GEM5 confirms that LUC have significantly more impact on wind in orographic regions when TOFD is switched on (see annex /Wind/CHRQ exploratory analysis/). However, the direct effect of TOFD on roughness is difficult to understand. The aggregated value (level 5) of the momentum roughness length does not appear to change between simulations with or without TOFD. This is properly due to a misunderstanding of which roughness fields the model uses.

4.3.3.2. Wind speed distribution and atmospheric stability

Under very stable atmospheric conditions (e.g., cold regions and/or at night), there is a risk of decoupling between the surface and the atmosphere above. This may lead to severe inaccuracies and numerical instability, and therefore models have different ways of limiting stability. For instance, CRCM5 imposes a minimum wind speed in order to sustain some mixing, whereas CRCM6 imposes a minimum Obukhov length which directly limits how stable the atmosphere may become. According to Dr. Stéphane Bélair, these two approaches are equally justifiable from a physics standpoint. Both are tunable and therefore may be better or worse depending on the parameters chosen and the variable to be represented. Whittaker et al. (2024) evaluated the performance of CRCM6 for representing near-surface winds. They found that using a minimum wind speed instead of a minimum Obukhov length improves the match with observations from AmeriFlux stations.

Over the course of this analysis, however, it came to be suspected that imposing a minimum wind speed may lead to a spurious 'pile up' of low speeds in wind distributions. Take, for example, the GRASS wind distributions from Figure 27. Both locations picked at random show a bump at low wind speed. Why is the distribution bimodal and not a classic Weibull distribution? One can imagine that imposing a minimum wind speed could alter the low wind speed distribution in a non-realistic way.

In an exploratory analysis comparing CRCM5 with CRCM6-GEM5 (which uses a minimum Obukhov length by default), it was noticed anecdotally that low wind speed peaks are seen in CRCM5 but not in CRCM6-GEM5 (see annex: Analysis/Wind/). For instance, Figure 33 shows distributions at two random locations for the two models, with configurations chosen to be as close to each other as possible except for how they deal with stability. Compared with CRCM6-GEM5, CRCM5 exhibits a lack of wind speed occurrences below 1 m/s, and an excess between 1 and 2 m/s.

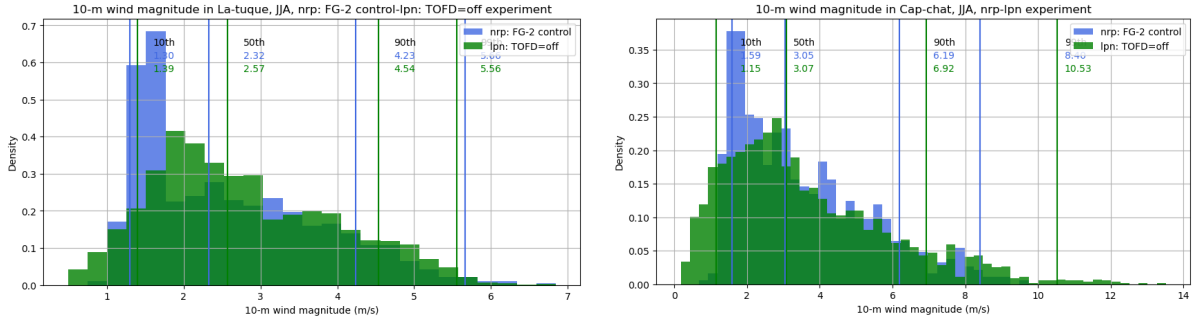

Figure 31 : Wind speed distribution in JJA for La Tuque and DJF for Cap-Chat using CRCM5 (blue) and CRCM6 (green). Both simulations are forced by ERA5, with no turbulent orographic form drag (TOFD).

Of course, CRCM5 and CRCM6 do not only differ by how they deal with strong stability. The exploratory analysis, among other things, also points to large changes in roughness which are difficult to pinpoint. Stability functions are also different, but these seem to have more minor effects over land. Nevertheless, if low wind speeds matter in future analyses of the ASIMLUC dataset, this potentially spurious 'pile-up' at low wind speed should be investigated more thoroughly.

4.3.4. Outlook on ASIMLUC winds

4.3.4.1. Is it worth pursuing the analysis of ASIMLUC wind?

The ASIMLUC dataset provides a unique opportunity to assess the impacts of LUC on near-surface wind. Several LUC scenarios are available, and the multiplicity of ensemble members allows for a reasonable account of internal variability. Section 4.3.2 outlines a few key results from the exploratory analysis.

However, it is not obvious this line of work is worth pursuing, and if so, in what direction. First, section 4.3.3 highlights important limitations regarding the ability of CRCM5 to accurately represent winds, in particular how they are affected by LUC. Notably, CRCM5 neglects changes in vegetation roughness in orographic regions. As a result, even the large-scale deforestation under SSP3-7.0 has little impact on the wind in the east coast of the US. There is also a reasonable doubt regarding the ability of CRCM5 to represent low wind speeds. Finally, wind energy applications would be complicated because ASIMLUC data is only available on pressure levels. Since all of the aforementioned limitations will be resolved in Ouranos' future CRCM6-GEM5-CMIP6 simulation ensemble, it is tempting to wait for this new dataset before carrying out an in-depth analysis. Note, however, that the LUC signal will be harder to isolate in this ensemble because land cover will likely evolve yearly.

4.3.4.2. A summary of lessons learned

We conclude this section with three technical lessons learned from the study of winds with CRCM5-CLASS.

Model output on pressure levels is suboptimal for wind energy applications. Use hybrid levels.

For most climate science applications, variables are output on constant pressure levels. This requires interpolation, as CRCM5-CLASS uses hybrid coordinates internally, which are a blend of hydrostatic pressure and height coordinate modified to follow terrain. Output of model data directly on hybrid levels is preferable for wind energy applications, where one is interested in conditions at the (fixed) height of a wind turbine.

Roughness changes due to LUC must be interpreted with caution in mountainous regions.

By default, CLASS computes an "effective roughness" equal to the maximum of vegetation and orographic roughness: vegetation roughness is ignored if topographic roughness is greater (and vice versa). Hence, LUC may have no impact on roughness in mountainous regions. This potential issue is resolved with the use of a turbulent orographic form drag (TOFD) parameterization, as is activated by default in CRCM6-GEM5.

Imposing a minimum wind speed may be skewing the wind profile in CRCM5

CRCM5 avoids the potential decoupling of the atmosphere from the surface in very stable regimes by imposing a minimum wind speed. It appears that this condition is causing a spurious 'pile up' of wind data at low speeds. This potential issue is resolved with the use of a minimum Obukhov length to limit atmospheric stability and avoid its decoupling from the surface, as is activated by default in CRCM6-GEM5.

4.4. FUTURE WORK

Several stones were left unturned over the course of ASIMLUC. Here we discuss avenues for future work. We begin with proposed technical work leveraging the outcomes of this project to improve the modeling system at Ouranos (section 4.4.1). We then outline some of the most promising opportunities for scientific inquiry (section 4.4.2), and end with a discussion on the importance of distilling the essence of this project for the benefit of end users and policy makers (section 4.4.3).

4.4.1. Opportunities for model improvement

4.4.1.1. Implementation of up-to-date land cover maps

During this project, it was realized that the land cover map used operationally at Ouranos is not from GLC2000, as was thought, but rather from the even older USGS-GLCC. On top of that, this so-called “legacy” land cover map was modified manually. It seems reasonable to suggest that the land cover map is due for an update.

The present-day LANDMATE cover map for North America has been implemented and validated with CRCM5 (see section 4.2.1.1). The next step will be to do the same with CRCM6-GEM5. While there is no guarantee that the results will be “better” with newer land cover products, we believe there is added value in adopting the state-of-the-art, if only to benefit by learning from other leading institutions using similar products.

4.4.1.2. Implementation of transient LUC

All simulations in this project were generated using static land cover. The biophysical effects of LUC were estimated by computing, for any variable of interest, the difference between simulations with different land maps (Figure 2). For instance, while we looked at realistic LUC scenarios ASIMLUC-II, we only compared simulations with present land cover (2015) and end-of-century land cover (2100) according to SSP1-2.6 or SSP3-7.0. This approach is analog to doubling or quadrupling CO_2 experiments used in the climate modeling community to estimate the sensitivity of climate models.

In reality, however, both greenhouse gas concentrations and land cover evolve smoothly in time. In the case of land cover, the changes are not even monotonous. For instance, under SSP1-2.6, cropland area in North America continues to decline until around 2060, when it starts rapidly increasing again (Figure 32). Such interesting trends are completely ignored in ASIMLUC.

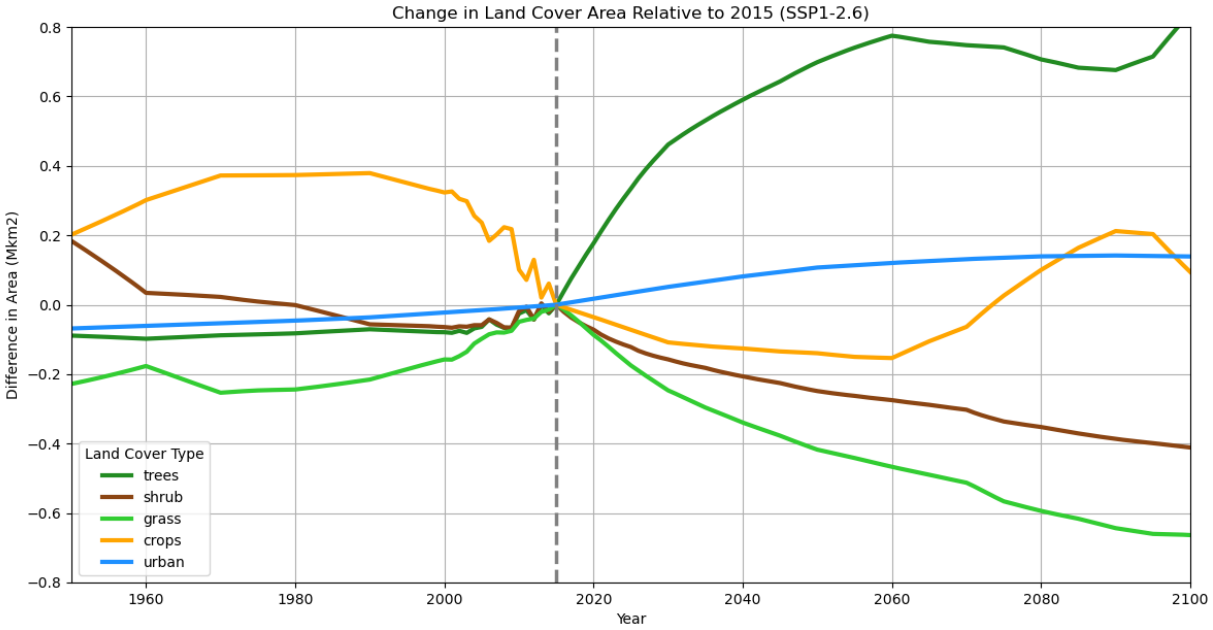

Figure 32 : Time series of the area spanned by different land cover types relative to 2015. Extension beyond 2015 according to scenario SSP1-2.6.

In CRCM5, greenhouse gas concentrations are specified yearly. It would be reasonable, as a first step, to also specify evolving land cover yearly. The yearly LANDMATE maps developed for this project make this possible (section 4.2.1). Accordingly, ongoing efforts at Ouranos aim to implement land cover maps changing yearly in CRCM6-GEM5. In the international community, the second phase of the LUCAS project is also producing its first simulations with yearly LUC. We recommend staying up to date with the LUCAS team to maximize learning.

4.4.1.3. Implementation of CLASSIC

The last proposed improvement is to implement the Canadian Land Surface Scheme Including Biochemical Cycles (CLASSIC). CLASSIC is the successor of its two component models: CLASS and the Canadian Terrestrial Ecosystem Model (CTEM). In fact, CLASS has not been updated independently for nearly a decade, and therefore to keep our model up to date we need to implement CLASSIC.

Aside from the adoption of a state-of-the-art model, two immediate benefits are worth mentioning. First, CLASSIC includes a stand-alone “shrub” vegetation category. Despite their relatively modest coverage, shrubs have an outsized influence on the surface energy balance given their strong stomatal resistance (section 4.2.3.1). At the moment, shrubs are awkwardly split into the broadleaf tree and grasses categories of CLASS, which is suboptimal.

The second benefit of CLASSIC is to allow for a more dynamic representation of vegetation. All biophysical properties are fixed in CLASS, except perhaps leaf-area index (LAI) for trees. For instance, broadleaf trees transition from dormant (minimum LAI) to fully-leafed (maximum LAI) over a period of thirty days triggered by near-zero air and top soil temperatures. In CLASSIC, vegetation properties can respond more holistically to climate and atmospheric conditions, temperature, water availability and CO_2 concentration.

4.4.2. Opportunities for scientific inquiry

4.4.2.1. LUC and precipitation: mechanisms and extremes

There is clear precipitation enhancement following large-scale forestation in both phases of the ASIMLUC dataset, and on both continents (Asselin et al., 2022, 2024). This widespread phenomenon is key to understanding the effects of LUC on the water cycle, including water availability. Yet, the mechanisms linking LUC and precipitation remain elusive. These mechanisms were briefly investigated in the FOREST-GRASS simulations over North America during a summer internship (section 4.1.3). The scientific literature was surveyed, and some of the plausible mechanisms identified do appear to be at play in the simulations analyzed. A next step would be to look at the effects of forestation under SSP1-2.6 in North America to see how well the conclusions hold in a more complex LUC scenario.

Beyond climatological means, do LUC also influence *extremes* of precipitation? Again, the same summer internship has briefly touched on this, finding increased strong summer precipitation following complete afforestation of North America (section 4.1.3). Are these effects also present under realistic scenarios such as SSP1-2.6? Are they also present in Europe?

Continent	FOREST-GRASS	SSP1-present	SSP3-present
NA	Mean: A22, I23 Extremes: I23	Mean: M25 Extremes: ...	Mean: M25 Extremes: ...
EU	Mean: A22 Extremes: ...	Mean: A24 Extremes: R	Mean: A24 Extremes: R

Figure 33 : A summary of reports on climatological mean and extreme precipitation for the ASIMLUC dataset. A22: Asselin et al. (2022). A24: Asselin et al. (2024). M25: Masters project to be concluded in 2025. I23: Internship of summer 2023. R: this report, section 4.2.2.3.

Figure 33 summarizes reports of climatological and extreme precipitation in the ASIMLUC dataset. It would be beneficial to assemble these analyses and fill the banks to reach a better understanding of the phenomenon. Yes, forests enhance precipitation recycling on average over 30 years, but if they also increase extreme precipitation significantly, that's another story.

4.4.2.2. Wind energy in Texas

As briefly discussed in section 4.3.2.3, we found that strong GHG emissions caused an increase in wind speed in Texas. It is not the first time that such a feature is reported, indicating that it may be a plausible signal. Given the societal importance of wind energy in this region, it would be worthwhile to explore this further.

However, the Ouranos operational ensemble might seem better suited than ASIMLUC-II for this task. The Ouranos CMIP6-CRCM5 ensemble comprises more GCMs and GHG scenarios and as many members as ASIMLUC-II for the MPI-ESM. If the Texas wind hot-spot does appear in this ensemble, it will be further reason to analyze it in full depth. In such case, the important limitations of wind representation in CRCM5 (section 4.3.3)

have to be considered carefully. Another option is to wait for the next CRCM6-GEM5 ensemble, for which wind will be thoroughly validated. On top of that, the next CRCM6-GEM5 will include wind data on hybrid levels, which are ideal for analyzing wind energy.

4.4.2.3. Solar energy potential

The energy transition requires vast increase in renewable energy production, with wind and solar projected to account for most of the growth. So far, we mostly focused on the effects of LUC on wind energy (section 4.3), but it would be valuable to at least explore its effects on solar energy as well.

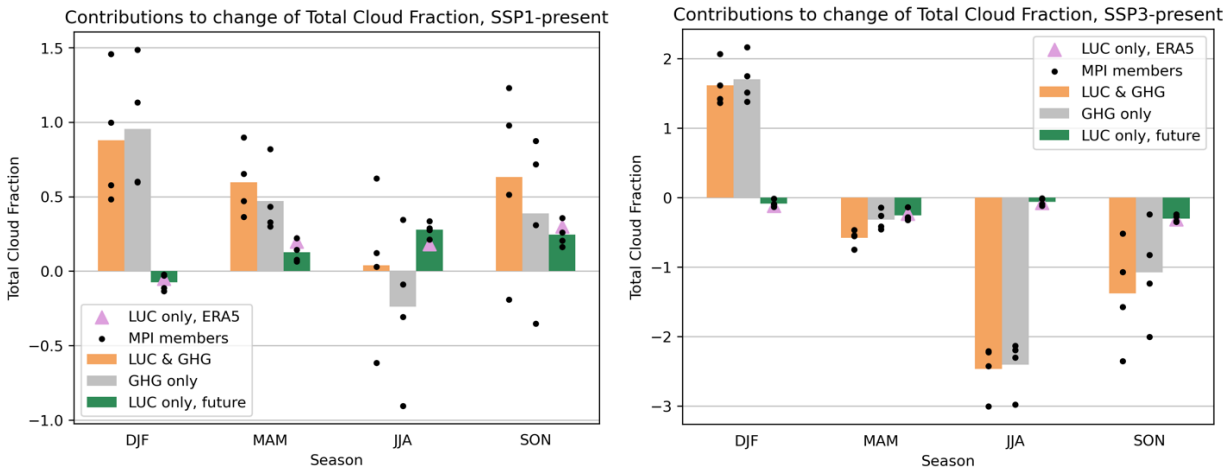

Figure 34: Changes in cloud cover over Europe for scenarios SSP1-2.6 and SSP3-7.0.

Figure 34 shows the relative contribution of GHG and LUC to cloud coverage over Europe under SSP1-2.6 (left) and SSP3-7.0 (right). In the former scenario, LUC increase average cloud cover by a few tens of a percent during summer and fall, which is comparable with the GHG effect, although not necessarily in the same direction. What is the impact of such a cloudiness change on incident shortwave radiation? Are changes in solar input felt more strongly over solar-rich or solar-poor regions? Are changes to surface temperature important for the performance of solar panels?

4.4.2.4. Neglected LUC scenarios

Historical LUC

None of the (two) simulations with historical land cover have been analyzed so far (blue table in Figure 8). Yet, analyzing the effects historical LUC may offer an avenue for engaging effectively with the wider public. What is the role of historical LUC on present climate and hydrology? In other words, how did our past action shape the present? These could be helpful nuggets of information to start a discussion, for instance, with policy makers.

SSP3-7.0 over Europe

The effects of LUC under SSP3-7.0 in Europe have received little attention so far. The exploratory of LUC effects in Europe (section 4.2.2) did touch upon SSP3-7.0, but none of the results were published. While it is true that LUC effects are generally much weaker than that of GHG emissions in this scenario (Figure 17), there is still an interesting message emerging from this analysis and which differs qualitatively from LUC under SSP1-2.6

(section 4.2.3; Asselin et al. 2024). While large-scale forestation under SSP1-2.6 mitigates heat waves, 'shrubification' of cropland under SSP3-7.0 tends to exacerbate heat by inhibiting evapotranspiration, and hence it amplifies the effects of global warming.

4.4.2.5. LUC, roughness and wind in Europe

Analysis of Europe simulations has been carried out without knowing about effective roughness (section 4.3.3.1). We now know that orography interferes with the roughness signal of LUC, with potentially important consequences (section 4.2.4.3). One first step would be to look into roughness changes in Europe. How does it compare to North America? Could this help deepen our understanding of LUC effects in Europe, such as why the broadleaf-to-crops transition in southwest Russia is associated with increased evapotranspiration?

4.4.2.6. Natural climate variability

Another severely untapped resource is the multiplicity of ensemble members. Inter-member variability was mainly used to assess the statistical robustness of the LUC sensitivity analysis. Yet, there are several variables whose variability is of high interest. For instance, an interesting avenue would be to look at precipitation, for which variability is significant and the link with LUC is present but hard to elucidate with climatological means. Assessing the impact of LUC on temperature interannual variability and the amplitude of the daily cycle could be of interest as well.

4.4.2.7. Hydrological studies

LUC are of primary interest in the field of hydrology. Of course, the flow of water depends on the type of land cover, and therefore LUC scenarios may have direct consequences on hydrological extremes such as floods. On top of that, we learned over the course of this project that LUC may influence all main climatic drivers of hydrology: precipitation, temperature, radiation, wind, humidity, etc. As such, the ASIMLUC dataset is a great tool for studying the effects of LUC and GHG on hydrology.

Teams of hydrologists based at the École de Technologie Supérieur (ETS) and at the Ludwig-Maximilians-Universität München (LMU) are currently using the ASIMLUC dataset for a variety of applications. For instance, the team of Annie Poulin at ETS is looking at the influence of extreme LUC on peak flow in Québec using ASIMLUC-I (section 4.1.4). Jean-Luc Martel at ETS is proposing to use long-short-term memory (LSTM) neural networks to learn how LUC impact hydrology using ASIMLUC-II. The LMU team is working on multivariate bias correction of ASMILUC-II before feeding it into their hydrological model, WaSiM.

Preliminary results from Annie Poulin's group suggest that hydrological models such as HYDROTEL and WaSiM represent land cover rudimentarily (section 4.1.4). The setup of their study is traditional: hydrological models are fed CRCM5 or ERA5 data for daily temperature minima and maxima along with precipitation. Complex phenomena such as snow dynamics, evapotranspiration, infiltration and run-off are dealt with internally by the hydrological models. Yet, it seems likely that land surface models such as CLASS could simulate these processes more accurately. Why, then, would one outsource these phenomena to a more rudimentary model?

Stand-alone LSMs like CLASS or CLASSIC cannot produce hydrographs like HYDROTEL. The main missing piece is a routing scheme. In CLASS, for example, runoff is generated at individual grid points and essentially

vanishes from the model without interacting with neighboring points. A routing scheme would allow this runoff to be channeled across the landscape, connecting multiple grid points to simulate the movement of water through river networks. By coupling CLASS with a hydrological routing model, it then becomes possible to produce hydrographs comparable to with outputs of HYDROTEL or other hydrological models.

This is a non-trivial undertaking that will be carried out in the Ouranos project "*Prise en compte de l'incertitude de modélisation hydrologique dans la caractérisation des zones inondables en climat futur*", led by David Huard and Louise Arnal. The idea is to first work from the Surface Prediction System (SPS), an uncoupled surface version of CRCM which can be used in conjunction with a variety of LSMs. Runoff produced by the LSM, which might require post-treatment such as bias correction, can then be fed to a river routing scheme (e.g., using Raven). Comparing output from this modeling chain to the more traditional approach used at ETS may prove insightful. Which approach matches observations of evapotranspiration, snow and streamflow better?

4.4.2.8. Exploring surface model parameters

Land surface models such as CLASS comprise a slew of parameters. In this project, we performed all simulations with a single set of parameters. How confident are we that the phenomena of interest were optimally represented by this parameter set? An interesting avenue for future work would be to explore more systematically the parameter space in CLASS. Parameter exploration would help us quantify the contribution of the LSM to uncertainty (which we know to be crucial from LUCAS). Similar experiments on RCMs yielded dramatic improvements in performance, so it is possible that parameter optimization in CLASS could also be highly beneficial.

4.4.2.9. Urban Climate

The expansion of cities is a type of LUC we have not considered seriously in the course of this project. The rationale is that changes in urban area tend to be small compared with (de)forestation and cropland expansion and abandonment (e.g., Figure 7), and therefore their regional effects are relatively weak. Yet, most people now live in cities, and therefore the effects of climate are overwhelmingly felt on these small (~1%) regions of the Earth's surface.

At the time of writing, CRCM5-CLASS basically treats cities as rock: "urban" is a land cover category but it has generic biophysical properties which ignore the high complexity of urban area. The Town Energy Balance (TEB) urban model exists in the source code, but it is not activated. Careful implementation of TEB would require assistance from experts, and validation would benefit from an intercomparison project such as the LUCAS FPS for LUC. Fortunately, there is a new CORDEX FPS doing exactly that: the URBan environments and Regional Climate Change (URB-RCC) project. Yours truly participated in a *Urban Climate* paper describing the initiative:

"*Towards better understanding the urban environment and its interactions with regional climate change - The WCRP CORDEX Flagship Pilot URB-RCC*" by Gaby Langendijk, Tomas Halenka, Peter Hoffmann, Marianna Adinolfi, Aitor Aldama Campino, Olivier Asselin, Sophie Bastin, Benjamin Bechtel, Michal Belda, Angelina Bushenkova, et al. (see annex: /Publications/Scientific Papers/).

The core idea of Langendijk et al. (2024) is to get modeling centers to agree on a simulation protocol that will facilitate comparison between different RCMs and urban models. Unfortunately, as in the case of LUCAS, we are running late. First-phase simulations of URB-RCC are already ongoing, but the implementation of TEB in CRCM5-CLASS is merely at the planning phase. It would be valuable to invest time earlier than later in order to catch up to the international community.

4.4.3. Opportunities for outreach

This report is admittedly quite technical for common climate data users. In part, this is because the science of LUC effects on climate and hydrology is still at an early stage. While the fundamentals are fairly well understood, inter-model divergence is alarming and thus predicting quantitatively the local and non-local effects of LUC remains elusive in the near-term.

It emerged as a consensus among members of our follow-up committee, however, that the science needs not be fully settled before starting a conversation with the public. While scientific debate rages at the bleeding edge, there is relatively good confidence on some basic results. For instance, we can definitely assert that LUC can impact climate and hydrology. The first step may be to simply raise awareness regarding the potential effects of LUC. The message could be as basic as highlighting that LUC can affect temperature and precipitation.

Aside from publishing papers in scientific journals, we made two attempts at dissemination (section 4.1.5): facilitating a panel on forest-climate interactions at the Ouranos Symposium and writing a popular science paper on the role of trees in combating climate change. We also made a particular effort to frame the results of ASMILUC-II around impacts that matter to humans. Asselin et al. (2024), which showed how large-scale forestation impacts heat waves and water availability (section 4.2.3), was a step in the right direction, but remains still quite opaque to most end users. Another way to engage the wide public could be to focus on sector-specific impacts of LUC. For instance, a case study on the effects of LUC on wind energy potential in Quebec could help illustrate how LUC can matter.

While GHG emissions come from numerous sources worldwide and their effects are globally diffused due to atmospheric mixing, the impacts of LUC are often more localized. This presents an opportunity for local policies to mitigate or harness these effects, making them particularly relevant for policy makers at all levels of government—from municipal to federal.

5. Conclusion

The contemporary conversation on climate change (rightly) gravitates around greenhouse gas (GHG) emissions. However, these emissions are not the only way human activities drive climate change. Land-use changes (LUC), such as deforestation and cropland expansion, alter transfers of energy and water between Earth's surface and the atmosphere. These so-called biophysical effects of LUC are the focus of this Assessment of the Impacts of Land-Use Changes on climate (ASIMLUC). There is mounting evidence that the biophysical effects of LUC can dominate the more diffuse effects of GHG emissions at regional scales. Paradoxically, while LUC are typically included in coarse-resolution global climate models (GCMs), no regional climate model (RCM) takes LUC into account operationally.

International efforts such as LUCAS aim to resolve this paradox by coordinating intercomparison projects and guide implementation of LUC in RCMs. In ASIMLUC-I, we contributed to this European project and expanded it to North America (section 4.1.1). LUCAS was a perfect setting to learn about the sensitivity of CRCM5-CLASS to extreme LUC and compare its performance to the other leading RCMs and land surface models (LSMs). In essence we found that CRCM5-CLASS sits well within the LUCAS ensemble of RCMs/LSMs for the summertime temperature response, but note that it produces the most extreme winter warming amplitude of all LUCAS models (Figure 10).

In the second phase of this project, we considered realistic LUC scenarios. The first step was to generate land cover maps representative of various socio-economic pathways in collaboration with colleagues from the LUCAS team (section 4.2.1). The simulation ensemble over Europe was produced and analyzed first (section 4.2.2). A systematic exploration of the relative contributions of GHG and LUC to various key variables showed that LUC have the most impact of extreme temperatures, turbulent heat fluxes and water fluxes, especially during summertime in SSP1-2.6. Accordingly, the main paper from ASIMLUC-II focused on the role large-scale forestation in mitigating extreme heat at the expense of water availability (section 4.2.3).

So far, comparatively less work has been done on the ASIMLUC-II ensemble over North America, because the land cover maps were available only later. The major ongoing analysis focuses on how LUC impact the water cycle in North America (section 4.2.4). As a bridge to a project with the Centre de Recherche d'Hydro-Québec (CHRQ) on wind under climate change, we analyzed wind data in both phases of ASIMLUC (4.3). This exercise proved equally frustrating and insightful. On the one hand, severe limitations were highlighted which reduced confidence in the wind data analyzed (section 4.3.3). On the other hand, these difficulties are highly informative for the wind energy work to come.

Several avenues for future work were highlighted and discussed in section 4.4. For instance, we believe it would be beneficial to pursue work on how LUC influence precipitation, especially their extremes. A related low-hanging fruit is the study of LUC influence on solar energy via changes in cloud coverage and incident shortwave radiation. For wind energy, however, it may be wiser to wait for the next-generation CRCM6-GEM5 ensemble with its hybrid-level output and various other fixes (section 4.3.4). We also explore, with genuine dilettantism, promising avenues for hydrological research utilizing CLASS with expanded capabilities to route water and produce hydrographs comparable to traditional hydrological models. Finally, we highlight the relevance of integrating urban processes in the modeling system at Ouranos.

References

Asselin, O., Leduc, M., Paquin, D., de Noblet-Ducoudré, N., Rechid, D., & Ludwig, R. (2024). Blue in green: forestation turns blue water green, mitigating heat at the expense of water availability. *Environmental Research Letters*, *19*(11), 114003. https://doi.org/10.1088/1748-9326/ad796c

Asselin, O., Leduc, M., Paquin, D., Di Luca, A., Winger, K., Bukovsky, M., Music, B., & Giguère, M. (2022). On the Intercontinental Transferability of Regional Climate Model Response to Severe Forestation. *Climate*, *10*(10), 138.

Davin, E. L., Rechid, D., Breil, M., Cardoso, R. M., Coppola, E., Hoffmann, P., Jach, L. L., Katragkou, E., de Noblet-Ducoudré, N., Radtke, K., & others. (2020). Biogeophysical impacts of forestation in Europe: first results from the LUCAS (Land Use and Climate Across Scales) regional climate model intercomparison. *Earth System Dynamics*, *11*(1), 183–200.

de Noblet-Ducoudré, N., Boisier, J.-P., Pitman, A., Bonan, G. B., Brovkin, V., Cruz, F., Delire, C., Gayler, V., den Hurk, B., Lawrence, P. J., & others. (2012). Determining robust impacts of land-use-induced land cover changes on surface climate over North America and Eurasia: Results from the first set of LUCID experiments. *Journal of Climate*, *25*(9), 3261–3281.

Hoffmann, P., Reinhart, V., Rechid, D., de Noblet-Ducoudré, N., Davin, E. L., Asmus, C., Bechtel, B., Böhner, J., Katragkou, E., & Luyssaert, S. (2023). High-resolution land use and land cover dataset for regional climate modelling: Historical and future changes in Europe. *Earth System Science Data*, *15*(8), 3819–3852.

IPCC, 2019: Climate Change and Land: an IPCC special report on climate change, desertification, land degradation, sustainable land management, food security, and greenhouse gas fluxes in terrestrial ecosystems [P.R. Shukla, J. Skea, E. Calvo Buendia, V. Masson-Delmotte, H.-O. Pörtner, D. C. Roberts, P. Zhai, R. Slade, S. Connors, R. van Diemen, M. Ferrat, E. Haughey, S. Luz, S. Neogi, M. Pathak, J. Petzold, J. Portugal Pereira, P. Vyas, E. Huntley, K. Kissick, M. Belkacemi, J. Malley, (eds.)]. In press.

Johnson, D. L., & Erhardt, R. J. (2016). Projected impacts of climate change on wind energy density in the United States. *Renewable Energy*, *85*, 66–73.

Langendijk, G. S., Halenka, T., Hoffmann, P., Adinolfi, M., Aldama Campino, A., Asselin, O., Bastin, S., Bechtel, B., Belda, M., Bushenkova, A., Campanale, A., Chun, K. P., Constantinidou, K., Coppola, E., Demuzere, M., Doan, Q. Van, Evans, J., Feldmann, H., Fernandez, J., … Yuan, J. (2024). Towards better understanding the urban environment and its interactions with regional climate change - The WCRP CORDEX Flagship Pilot Study URB-RCC. *Urban Climate*, *58*, 102165. https://doi.org/10.1016/J.UCLIM.2024.102165

Martynov, A., Laprise, R., Sushama, L., Winger, K., Šeparović, L., & Dugas, B. (2013). Reanalysis-driven climate simulation over CORDEX North America domain using the Canadian Regional Climate Model, version 5: model performance evaluation. *Climate Dynamics*, *41*(11), 2973–3005.

Meier, R., Schwaab, J., Seneviratne, S. I., Sprenger, M., Lewis, E., & Davin, E. L. (2021). Empirical estimate of forestation-induced precipitation changes in Europe. *Nature Geoscience*, *14*(7), 473–478.

Mioduszewski, J., Vavrus, S., & Wang, M. (2018). Diminishing Arctic sea ice promotes stronger surface winds. *Journal of Climate*, *31*(19), 8101–8119.

Perugini, L., Caporaso, L., Marconi, S., Cescatti, A., Quesada, B., de Noblet-Ducoudre, N., House, J. I., & Arneth, A. (2017). Biophysical effects on temperature and precipitation due to land cover change. *Environmental Research Letters*, *12*(5), 53002.

Pryor, S. C., & Barthelmie, R. J. (2011). Assessing climate change impacts on the near-term stability of the wind energy resource over the United States. *Proceedings of the National Academy of Sciences*, *108*(20), 8167–8171.

Pryor, S. C., Barthelmie, R. J., Bukovsky, M. S., Leung, L. R., & Sakaguchi, K. (2020). Climate change impacts on wind power generation. *Nature Reviews Earth & Environment*, *1*(12), 627–643.

Rechid, D., Davin, E., de Noblet-Ducoudré, N., Katragkou, E., & the LUCAS team. (2017). CORDEX Flagship Pilot Study" LUCAS-Land Use & Climate Across Scales"-a new initiative on coordinated regional land use change and climate experiments for Europe. *EGU General Assembly Conference Abstracts*, 13172.

Reinhart, V., Hoffmann, P., Rechid, D., Böhner, J., & Bechtel, B. (2022). High-resolution land use and land cover dataset for regional climate modelling: a plant functional type map for Europe 2015. *Earth System Science Data*, *14*(4), 1735–1794.

Riahi, K., van Vuuren, D. P., Kriegler, E., Edmonds, J., O'Neill, B. C., Fujimori, S., Bauer, N., Calvin, K., Dellink, R., Fricko, O., Lutz, W., Popp, A., Cuaresma, J. C., KC, S., Leimbach, M., Jiang, L., Kram, T., Rao, S., Emmerling, J., … Tavoni, M. (2017). The Shared Socioeconomic Pathways and their energy, land use, and greenhouse gas emissions implications: An overview. *Global Environmental Change*, *42*, 153–168. https://doi.org/10.1016/J.GLOENVCHA.2016.05.009

Šeparović, L., Alexandru, A., Laprise, R., Martynov, A., Sushama, L., Winger, K., Tete, K., & Valin, M. (2013). Present climate and climate change over North America as simulated by the fifth-generation Canadian regional climate model. *Climate Dynamics*, *41*(11), 3167–3201.

Verseghy, D. L. (1991). CLASS—A Canadian land surface scheme for GCMs. I. Soil model. *International Journal of Climatology*, *11*(2), 111–133.

Verseghy, D. L., McFarlane, N. A., & Lazare, M. (1993). CLASS—A Canadian land surface scheme for GCMs, II. Vegetation model and coupled runs. *International Journal of Climatology*, *13*(4), 347–370.

Wang, A., Price, D. T., & Arora, V. (2006). Estimating changes in global vegetation cover (1850–2100) for use in climate models. *Global Biogeochemical Cycles*, *20*(3). https://doi.org/10.1029/2005GB002514

Wang, L., Arora, V. K., Bartlett, P., Chan, E., & Curasi, S. R. (2023). Mapping of ESA's Climate Change Initiative land cover data to plant functional types for use in the CLASSIC land model. *Biogeosciences*, *20*(12), 2265–2282. https://doi.org/10.5194/bg-20-2265-2023

Wang, L., Bartlett, P., Pouliot, D., Chan, E., Lamarche, C., Wulder, M. A., Defourny, P., & Brady, M. (2019). Comparison and Assessment of Regional and Global Land Cover Datasets for Use in CLASS over Canada. *Remote Sensing*, *11*(19), 2286. https://doi.org/10.3390/rs11192286

Whittaker, T., Di Luca, A., Roberge, F., & Winger, K. (2024). Evaluating near-surface wind speeds simulated by the CRCM6-GEM5 model using AmeriFlux data over North America. *ArXiv Preprint ArXiv:2408.15932*.

Wohland, J. (2022). Process-based climate change assessment for European winds using EURO-CORDEX and global models. *Environmental Research Letters*, *17*(12), 124047.

Wohland, J., Hoffmann, P., Lima, D. C. A., Breil, M., Asselin, O., & Rechid, D. (2024). Extrapolation is not enough: impacts of extreme land use change on wind profiles and wind energy according to regional climate models. *Earth System Dynamics*, *15*(6), 1385–1400. https://doi.org/10.5194/esd-15-1385-2024

Zapponini, M., & Goessling, H. F. (2024). Atmospheric destabilization leads to Arctic Ocean winter surface wind intensification. *Communications Earth & Environment*, *5*(1), 262.

List of Figures

Figure 1 : LUC trump greenhouse gas emissions in mitigating summer heat extremes by the end of the century under SSP1-2.6. The three panels show the respective contributions of LUC, greenhouse gas emissions and their sum to summer heat extremes, defined by the 95th percentile of maximum daily temperature over the months of June, July and August (Asselin et al. 2024). 4

Figure 2 : Illustration of the methodology used in this project. Global climate data, which may come from reanalyses or global climate models, is downscaled dynamically over a given continent and period. Regional climate simulations with different configurations (e.g., land cover maps) are compared to assess the effect of this change on a variable of interest (e.g., temperature)..... 9

Figure 3: Land cover maps for ASIMLUC-I: FOREST and GRASS. 10

Figure 4: The expanded LUCAS simulation ensemble. Each square corresponds to a trio of simulations (FOREST, GRASS and control) for a unique RCM/LSM combination. Green squares depict the original LUCAS ensemble described in Davin et al. (2020). Blue squares depict the ensemble produced in the first phase of ASIMLUC. 11

Figure 5: LANDMATE land cover maps in the present (2015), and LUC between 2015 and 2100 for SSP1-2.6 and SSP3-7.0. 13

Figure 6 : LANDMATE land cover maps in the present (2015), and LUC between 2015 and 2100 for SSP1-2.6 and SSP3-7.0. 13

Figure 7 : Spatially-integrated land-use changes between 2015 and 2100 for both continents and both scenarios. The bar graphs show the sums of all positive (pale green) and all negative (pale purple) changes as well as the net change (dark green or purple)..... 14

Figure 8: Simulation ensemble for ASIMLUC-II (for both North America and Europe). The four green tables represent the ensemble forced by the four MPI-ESM members. There are five model configurations with different combinations of GHG and land covers, times 4 members. The blue table represents the ERA5-driven ensemble..... 15

Figure 9: Illustration of main mechanisms driving the temperature response to extreme LUC. Left: albedo-driven warming in winter and spring. Right: evapotranspiration-driven cooling in the summer. 16

Figure 10 : Summary of the CRCM5-CLASS response to extreme afforestation/deforestation and comparison with LUCAS ensemble, based on Asselin et al. (2022)..... 17

Figure 11 : Near-surface temperature and surface albedo effects of LUC during winter (DJF). The dark blue contour indicates significant (20%) snow cover. Correlations are computed over regions with both significant LUC (>5%) and snow cover. Upper panels: SSP1-present LUC; lower panels: SSP3-present LUC. 27

Figure 12: Left : January albedo for dominant CLASS categories (>50% of cover) as a function of snow depth. Averaged over 1986-2015 over present climate and land cover. Right : monthly latent heat fluxes over dominant land covers. 28

Figure 13: Key variables for the summertime (JJA) response to LUC in SSP1. From top left to bottom right: near-surface temperature, precipitation, latent minus sensible heat fluxes, shrubland change, net shortwave radiation, cloud fraction, surface albedo and needleleaf tree change. Correlations added to the maps are computed between the variable shown in the map and that which appears in the subscript of R. For instance, R_{tas} in the SW panel means that there is a Pearson correlation coefficient of 0.39 between SW and near-surface temperature over regions of significant LUC. 28

Figure 14 : Key variables for the summertime (JJA) response to LUC in SSP3. From top left to bottom right: near-surface temperature, precipitation, latent minus sensible heat fluxes, shrubland change, net shortwave radiation, cloud fraction, surface albedo and cropland change. 29

Figure 15: Relative contributions of GHG (grey), LUC (green) and both combined (gold) to latent heat fluxes. Values are averaged over all regions of significant LUC (>5%) in Europe. Small dots represent each of the four MPI-driven ensemble members, and pink triangles is associated with ERA5-driven runs. Left: SSP1-present; right: SSP3-present. 30

Figure 16: Relative contributions of GHG and LUC on latent heat fluxes under SSP1-2.6. Hatching shows regions of inter-model disagreement (half of the members give a positive delta, the other half a negative delta). 30

Figure 17: Relative contributions of GHG and LUC on a variety of variables. Upper row: SSP1-2.6. Lower row: SSP3-7.0. From left to right: temperature-related variables, surface energy balance components, moisture-related variables. Red squares mean that LUC-induced change to a given variable have an amplitude at least as great as GHG-induced changes to that same variable, and they share the same sign. Purple means the same, except that the LUC and GHG cause changes of different sign. Each row represents a scenario, and the three matrices assemble, from left to right, variables related to temperature, energy and water. 31

Figure 18: Changes to the 95th percentile of summertime daily minimum and maximum temperatures and precipitation due to GHG and LUC under SSP1-2.6. 32

Figure 19 : Changes to the 95th percentile of summertime daily minimum and maximum temperatures and precipitation due to GHG and LUC under SSP3-7.0. 33

Figure 20: Ensemble-averaged summertime (JJA) diurnal surface energy fluxes and temperature at site B, in the countryside near Budapest. The top row shows the climatology of the region, the bottom row shows the climatology for hot days only, defined as days with maximum temperature exceeding the 95th percentile. The left panels are the absolute fluxes and temperature in present-day climate and with present land cover. The right panels show the change in those quantities due to LUC. The pie charts in the left panels show the present-day land cover fraction: crops (orange), grass (yellow), pale green (broadleaf), shrubs (brown) and urban (grey). The bar graphs included in the right panels show the change between end-of-century and current land cover categories. Energy fluxes are shown in solid lines while temperature is represented by dashed lines. 36

Figure 21: LUC-induced changes for a few ensemble-averaged variables under SSP1-2.6. 39

Figure 22: LUC-induced changes to a few ensemble-averaged variables under SSP3-7.0. 41

Figure 23 : Changes in evapotranspiration and key related biophysical properties due to LUC under SSP3-7.0 on the eastern coast of North America. From left to right: changes in evapotranspiration, maximum and minimum leaf area index (LAI), root depth and minimum stomatal resistance. 42

Figure 24: Two-dimensional binned distribution of roughness and climatological surface wind speed changes for each of the three scenarios considered. Water bodies are not included. 44

Figure 25: Topographic roughness versus changes in tree fraction, roughness and climatological near-surface wind for LUC scenarios FOREST-GRASS (upper row), SSP1-present (middle row) and SSP3-present (lower row). 45

Figure 26 : Roughness, average wind and its 95th and 99th percentile for FOREST, GRASS and their difference. Maps are for wintertime (DJF). 46

Figure 27: Wind speed distributions at two specific locations for FOREST (green) and GRASS (gold) simulations. Left: Peawanuck, in Northern Ontario; right: Fargo, bordering North Dakota and Minnesota in the US Midwest. Vertical lines depict the 95th wind speed percentiles. 46

Figure 28: Change in the wind profile in FOREST-GRASS. Points, crosses and triangles represent average, 95th and 99th percentile wind speeds at different pressure levels. The distribution of heights above topography is depicted as bar graphs on the right axis. Each color represents a different pressure level. 47

Figure 29 : Left to right: height of the 950 hPa isobar above topography, average, 95th and 99th percentile of wind modulus at 950hPa. Masked values are below ground. Contour at 300 m above ground. 47

Figure 30: Effects of LUC and GHG on ensemble-averaged climatological wind speed in ASIMLUC-II. Changes are normalized by the control climatology. Statistically insignificant pixels are masked following a two-sided Wilcoxon rank-sum test. The p-values obtained were submitted to a Benjamini-Hochberg correction with a false discovery rate of 0.05. 48

Figure 31 : Wind speed distribution in JJA for La Tuque and DJF for Cap-Chat using CRCM5 (blue) and CRCM6 (green). Both simulations are forced by ERA5, with no turbulent orographic form drag (TOFD). 51

Figure 32 : Time series of the area spanned by different land cover types relative to 2015. Extension beyond 2015 according to scenario SSP1-2.6. 55

Figure 33 : A summary of reports on climatological mean and extreme precipitation for the ASIMLUC dataset. A22: Asselin et al. (2022). A24: Asselin et al. (2024). M25: Masters project to be concluded in 2025. I23: Internship of summer 2023. R: this report, section 4.2.2.3. 56

Figure 34: Changes in cloud cover over Europe for scenarios SSP1-2.6 and SSP3-7.0. 57

List of Acronyms

Acronym	Definition
ASIMLUC	Assessment of the impacts of land-use changes on climate (this project)
CCCma	Canadian Center for Climate Modelling and Analysis
CLASS	Canadian land surface scheme
CLASSIC	Canadian land surface scheme including biochemical cycles
CORDEX	Coordinated regional downscaling experiment
CRCM	Canadian regional climate model
CTEM	Canadian Terrestrial Ecosystem Model
DOI	Digital Object Identifier
DTU	Danish Technical University
ECCC	Environment and Climate Change Canada
ECMWF	European Center for Medium-Range Weather Forecast
ERA	ECMWF reanalysis
ESM	Earth system model
ETS	École de technologie supérieure
FG	FOREST-GRASS
FPS	Flagship Pilot Study
GCM	Global climate model
GHF	Ground heat fluxes
GHG	Greenhouse gas
LAI	Leaf area index
LANDMATE	LAND surface Modifications and its feedbacks on local and regional cliMATE
LH	Latent heat
LMU	Ludwig Maximilian University (Munich)
LRZ	Leibniz Supercomputing Center

LSM	Land surface model
LSTM	Long Short-Term Memory
LUC	Land-use changes
LUCAS	Land-use and climate across scales
LW	Longwave
MPI	Max Planck Institute
RCM	Regional climate model
SH	Sensible heat
SSP	Socio-economic pathway
SW	Shortwave
TEB	Town Energy Balance
TOFD	Turbulent Orographic Form Drag
URB-RCC	Urban Environments and Regional Climate Change

Ouranos
Consortium sur les changements climatiques

550, rue Sherbrooke O, Tour Ouest, 19e étage
Montréal (Québec) H3A 1B9

ouranos.ca